ITUPublications

International Telecommunication Union
Radiocommunication Sector

Report ITU-R RA.2126-2

(03/2026)

RA Series: Radio astronomy

Mitigation techniques relating to radio frequency interference into radio astronomy

Foreword

The role of the Radiocommunication Sector is to ensure the rational, equitable, efficient and economical use of the radio-frequency spectrum by all radiocommunication services, including satellite services, and carry out studies without limit of frequency range on the basis of which Recommendations are adopted.

The regulatory and policy functions of the Radiocommunication Sector are performed by World and Regional Radiocommunication Conferences and Radiocommunication Assemblies supported by Study Groups.

Policy on Intellectual Property Right (IPR)

ITU-R policy on IPR is described in the Common Patent Policy for ITU-T/ITU-R/ISO/IEC referenced in Resolution ITU-R 1. Forms to be used for the submission of patent statements and licensing declarations by patent holders are available from https://www.itu.int/ITU-R/go/patents/en where the Guidelines for Implementation of the Common Patent Policy for ITU-T/ITU-R/ISO/IEC and the ITU-R patent information database can also be found.

Series of ITU-R Reports

(Also available online at https://www.itu.int/publ/R-REP/en)

Series	Title
BO	Satellite delivery
BR	Recording for production, archival and play-out; film for television
BS	Broadcasting service (sound)
BT	Broadcasting service (television)
F	Fixed service
M	Mobile, radiodetermination, amateur and related satellite services
P	Radio-wave propagation
RA	**Radio astronomy**
RS	Remote sensing systems
S	Fixed-satellite service
SA	Space applications and meteorology
SF	Frequency sharing and coordination between fixed-satellite and fixed service systems
SM	Spectrum management
TF	Time signals and frequency standards emissions

***Note**: This ITU-R Report was approved in English by the Study Group under the procedure detailed in Resolution ITU-R 1.*

Electronic Publication
Geneva, 2026

REPORT ITU-R RA.2126-2

Mitigation techniques relating to radio frequency interference into radio astronomy

(2007-2013-2026)

TABLE OF CONTENTS

1 Introduction

Mitigation techniques fall into three general categories:

– Preventing radio frequency interference (RFI) signals from entering the astronomical data, including reduction of the Observatory's vulnerability to RFI signals (§ 4);

– Removing RFI signals from the data in real time (§§ 5.1, 5.2, 8.1, 8.2);

– Removing or reducing the impact of RFI offline, following completion of the observing (§§ 5.3, 5.4, 8.3, 8.4).

1.1 Definition and characteristics of radio frequency interference

To a radio astronomer, RFI is any unwanted addition to the cosmic signal that has the potential to degrade or prevent the successful conduct of an observation. The term RFI will be used in this sense throughout this Report. Unlike thermal noise, which has stable temporal stochastic properties (white noise) and can be dealt with through radiometric detection (i.e. long integration times and on-source minus off-source subtraction), an RFI signal is temporally, spatially or spectrally structured and can obscure a deep-space signal or produce a false positive detection.

1.2 Characteristics of astronomical signals

Astronomical signals are many factors of ten below the noise floor of the receiving system. Hence the power level at which RFI begins to be detrimental is far lower for radio astronomy than it is for other radiocommunication services. The variety of potential RFI sources is hence very large. They include personal wireless devices, radar glints from aircraft, satellite transponders, commercial broadcast services, automobile spark plugs and many others.

1.3 Dealing with radio frequency interference

The working assumption for most astronomical observations is that RFI-corrupted data are unusable, due to the inherent challenges in accurately removing RFI. At the same time, the increase in wireless communication services has resulted in a significant growth in RFI over the past few years. This

development provides powerful motivation to develop novel mitigation measures or techniques to flag or even excise RFI from datasets, enabling scientific usage of data that would otherwise be discarded. The aim of mitigation techniques is to enable astronomical observations to be conducted in increasingly used radio environments.

1.4 ITU documentation

The threshold levels of detrimental interference in radio astronomy bands are given in Recommendation ITU-R RA.769. The percentage of permissible data loss resulting from emissions above these thresholds is specified in Recommendation ITU-R RA.1513, applicable to all primary radio astronomy bands.

In the exclusive primary bands listed in Radio Regulations (RR) No. **5.340**, the so-called passive bands, all emissions are prohibited. Furthermore, RR No. **5.149**, contains frequency ranges used by the radio astronomy service (RAS) (also some without allocation) and administrations are urged to take all practicable steps to protect the RAS from harmful interference when assigning these frequency ranges to active-service spectrum users.

1.5 Adoption of mitigation methods

Despite much research on RFI mitigation over many years, methods other than filtering and simple excision of RFI-contaminated data are not at present widely used in radio astronomy. This lack of use is primarily because more complex forms of mitigation require costly hardware, challenging software development, and/or expert-user capability to exploit during or after an observation. In addition, different techniques need to be applied dependent on the type of astronomical source (e.g. continuum or spectral-line) hardware used, RFI encountered, and scientific goals of the dataset. Radio astronomers want to keep control over their data and are hesitant to adopt black box methods of mitigation. Though many mitigation techniques have been tested, it is not possible for any of them to address every issue posed by the diverse variety of RFI sources. Radio astronomy observations are made with many different aims that require a variety of different techniques and equipment.

1.6 Effective observing techniques

For many observing applications, the standard observing modes and signal processing techniques have provided an inherent degree of interference mitigation that proved adequate to obtaining useful astronomical data in the presence of some interference. Even in these cases, however, some information is lost. The standard observing techniques and their RFI mitigation effects are described here. Annex 1 provides further details and examples.

For aperture synthesis instruments, “fringe stopping” typically decorrelates the RFI received at widely-separated antennas. This fact tends to suppress the RFI in the associated correlation products [78], provided the signal is not received in the majority of antennae. In the case of some synthesis radio telescopes, such interference may still result in a spurious bright source appearing in the maps at the celestial pole, which makes high declination observations difficult or impossible.

Aperture array instruments, such as LOFAR in the Netherlands, have investigated advanced techniques such as spatial nulling [11]. This was considered because of its wide, full-sky field of view, its siting in well-populated regions, and its operation in unprotected HF and VHF bands that are crowded with broadcast and wireless radio services.

Perhaps the most vulnerable radio astronomy service (RAS) observations are those made with single-dish radio telescopes, as typically no “fringe stopping” decorrelation is available for these observers. The improvement in sensitivity to astronomical signals afforded by increasing integration time then leads to a proportional increase in sensitivity to RFI signals. The use of phased array and multi-feed

receivers on single dish telescopes to null RFI signals has been tested (Deshpande, 2011; Warnick, et al., 2009) [20a] [83a] but is not in common use.

Total power observations of pulsed phenomenon, such as are common for the observation of pulsars and fast radio bursts, require significant receiver bandwidth to achieve a useful signal-to-noise ratio. Large bandwidth receivers are also very vulnerable to strong transmitters outside of RAS bands, which can lead to saturation effects of the sensitive radio astronomy systems. The noise making up the astronomical signal is subject to frequency-dependent dispersion as it propagates through the rarefied plasmas in the interstellar medium. When observing a pulsed signal with a radio telescope, the pulse is deliberately de-dispersed using a combination of hardware and software, to recover an accurate (non-dispersed) representation of the intrinsic pulse profile. This process tends to reduce RFI, because the process of de-dispersing the pulsar signal consequently disperses the RFI (although the RFI still reduces the sensitivity of the observations). However, only limited mitigation is provided by these processes.

Data are always degraded when interference is present.

The impact of RFI extends beyond simply preventing or degrading certain observations or types of observation. It also limits the overall productivity of the radio astronomy station by making desirable observations prohibitively difficult or expensive in terms of observing time requirements, processing complexity and operational overheads.

2 RFI mitigation methodology – Layers of mitigation

As indicated in § 1, the techniques for data mitigation can be divided into three general categories. In any practical implementation, particular techniques are likely to be implemented at different stages in the data acquisition and processing. The technique to be used at any particular stage depends on the type of observation undertaken (e.g. single dish, single interferometer, interferometer network, phased-array) on the type of radio sources being observed, and on the scientific goal of the observations. The probable types of mitigation and stages at which it takes place are:

1) Pre-detection methods applied in the receiver system itself, possibly in connection with the data-taking backend.
2) Digital excision and RFI removal methods may be used before correlation. With the advent of software (SW) correlation, these digital methods may also be incorporated into the correlation process.
3) The application of digital methods after correlation and after data integration or data buffering.
4) Excision and/or flagging of the collected astronomical data to eliminate the effects of known and unknown sources of RFI.

The performance of all these methods depends on the interference-to-noise ratio (INR), i.e. on the strength of the RFI relative to the system noise, or on the ratio of system-noise variance to RFI variance. Most methods are only effective when the RFI is clearly detectable within the data and readily distinguishable from the scientific detections, and its effects can usually only be removed down to a level corresponding to the instantaneous noise. A figure of merit for these methods is the processing gain after RFI suppression or reduction, which can be expressed as the ratio of the signal-to-noise ratio (SNR) after processing to the SNR before processing.

The success of any technique depends on the required level of suppression and also on any loss of the signal-of-interest (SOI). The occupied bandwidth of an astronomical signal relative to that of the RFI must also be considered, particularly when considering the cumulative effects of mitigation from several stages. It is to be noted that each applied method can introduce a measure of toxicity

(i.e. damage to the data, especially to its statistical properties), which results in an incremental degradation of the data quality. The total damage done to data, as a measure of the data loss resulting from (subsequent) mitigation processing is quantified by the ratio of the SNR (after processing) to the SNR (in the absence of RFI).

3 Techniques for mitigating RFI

The development of techniques for mitigating RFI present in the analogue output of radio telescope receivers has been a rapidly developing field in recent years, spurred on by technological advances that enable real-time signal processing approaches to RFI mitigation. Helpful introductions are provided by review papers ([7], [37], [24], [15], [5], [51]), as well as in conference presentations and summaries presented under the RFI conference series[1].

For the purposes of this Report, a taxonomy of mitigation techniques follows:

1) *Pro-active measures*, to change the local RFI environment by means of regulatory or coordination measures. In addition, some modifications to receiving systems may be possible in some circumstances to exclude RFI from observational data by using filters and robust hardware designs.

2) *Spatial nulling*, or adaptive spatial filtering, mitigates persistent RFI by using array beam-forming techniques or the use of multi-antenna systems. Array beam-forming techniques orient pattern nulls towards sources of RFI. This distorts the nominal instrument beam pattern(s), but in many cases, such as when interference arrives from the direction of the deep sidelobe response, nulls can be formed with no loss of data from the signal of interest. Challenges include the difficulty of accurately estimating the spatial properties of interference, which limits the achieved null depth. Multi-antenna systems work similarly, here recording the RFI to allow for nulling or cross-correlation of the RFI signal.

3) *Waveform subtraction*, in the sense of "subtracting" RFI from the telescope output. This form of adaptive noise cancellation is potentially superior to temporal excision in the sense that the RFI is removed with no impact on the astronomy. This provides a "look through" capability that is nominally freed of the artifacts associated with a simple "cutting out" of data. In addition, methods that use the statistical properties of the data may achieve similar results. However, the trade-off with respect to temporal excision is usually that suppression is limited by the quality of the estimate of the interference received by the radio telescope.

4) *Anti-coincidence*, broadly meaning the discrimination of RFI by exploiting the fact that widely-separated antennas perceive identical astronomical signals, but differing RFI. Thus RFI makes a contribution to the background noise level at each antenna rather than to the correlated signals.

5) *Flagging in the temporal and frequency domain*, in the sense of "cutting out" RFI from the data. For example, RFI consisting of brief pulses in the time domain may be mitigated by blanking the data (or stopping the data taking process) when the pulse is present. In addition, digital methods allow flagging of RFI in both the time and frequency domains. A common property of all flagging techniques is the loss of astronomical data, with the possible distortion of the remaining data by artifacts introduced by the excision process or left over from the RFI signature.

[1] https://rfi-conference.org/

Though found frequently in the literature, using generic terms such as “cancelation” or “mitigation” to classify specific algorithms in the following discussion will be avoided since these descriptors can ambiguously refer to several of the categories listed above.

The pro-active methods are described in § 4. Spatial nulling (§ 5) and methods involving waveform subtraction (§ 6) have been demonstrated using real or simulated astronomical data, but are in most cases under further development and/or used only in special circumstances. Anti-coincidence techniques (§ 7) provide a very effective means for identifying data contaminated by RFI that cannot strictly be classified as mitigation, but are rather a means for identifying data that should be removed by temporal excision. Finally, mitigation methods that are frequently or routinely used at observatories are generally based on temporal data flagging, i.e. deletion of data that is believed to be contaminated by RFI. These methods are described in § 8.

4 Pro-active measures – Changing the RFI environment

4.1 Regulatory and coordination measures

Coordination with active users and the application of national and international regulations may reduce both the occurrence of RFI at a radio astronomy station and its impact on observations. Improving and strengthening the regulatory framework at national, regional, and international levels plays an important role in protecting passive use of the spectrum: resources in support of this approach are to be found in the ITU-R Handbook on Radio Astronomy (2013), Recommendations ITU-R RA.769 and ITU-R RA.1513, and the CRAF Handbook [19].

Coordination zones and radio quiet zones can be used to control RFI from terrestrial sources. Report ITU-R RA.2259 describes the general characteristics, requirements, and implementation considerations for a radio quiet zone, and provides, in its annexes, numerous examples of specific radio quiet zones. Many observatories have local and national regulations that prevent the installation of transmitters in the immediate proximity (within 2 to 6 km) of an observatory. Large-scale coordination and quiet zones have been implemented for several sites, such as the Mid West Radio Quiet Zone in Western Australia (MWRQZ, 2007), the National Radio Quiet Zone around Green Bank, WV (NRQZ, 1958) and the Puerto Rico Coordination Zone around the Arecibo Observatory, PR (PRCZ, 1998). The environments for telescopes, such as ALMA in Chile and the two sites for the Square Kilometre Array, are being controlled by forward-looking, national regulations to facilitate the most sensitive observations.

Since it is better to solve RFI issues before implementation, it is important to identify both existing and prospective new transmitters that may affect portions of the radio spectrum of interest to an observatory, keep up with changes in local licensing rules, and recognize trends in spectrum use. Spectrum monitoring may be used to identify nearby transmitters, to locate potential problems, and to perceive trends in the radio environment.

Radio quiet zones are subject to national legislation or rules, only, which means that they are not readily applicable to space-borne transmitters. However, as a mitigation technique (e.g. on a voluntary basis or subject to agreement between administrations), satellite systems often have the capabilities to implement certain exclusion areas. A prime example would be that satellites with active beamforming systems would avoid pointing their beams towards RAS stations in order to reduce the overall power received by the sensitive radio telescope systems.

4.2 Local measures

Experience shows that observatories are themselves often significant sources of RFI. Computing hardware and electronic installations required for the telescope buildings generate harmonic and

broadband emissions that can enter a telescope's detection system. Identification and elimination of interference from these sources is a high priority for every observatory. RFI-shielded cabinets and Faraday cages for electronics and computing equipment, as well as the reduction of human activity (remote observing) and limitations on the use of consumer electronics all contribute to making an observatory "radio-quiet" [71].

4.3 Pre-detection and post-detection measures

A standard method for reducing the impact of RFI in the frequency domain is to install a bandpass or high/low pass filter in a receiver, which results in an insertion loss and substantially raises the system temperature at frequencies close to a band-edge. Super-conducting filter technology can significantly decrease the impact of such filters, but is costly and very inflexible as these filters cannot be tuned in frequency. Filtering out strong signals outside the RAS allocations (but within the frequency range of the receiver) serves to prevent damage or saturation effects.

Much research has been applied to the design of robust receivers with a high degree of linearity, so that harsh RFI environments do not affect them. Broadband observations are possible when receiver systems are sufficiently linear that no aliasing occurs, no inter-modulation products are generated, and no overloading occurs [84] [85] [18] [79]. However, there will always be a target conflict between improving the robustness and the sensitivity of a receiver.

4.4 Operational data sharing

Radio telescopes are often located in remote locations in order to minimize the impact of anthropogenic radio sources. While provides massive benefits to reduce the RFI from terrestrial sources located close to the horizon of the RAS site, radio telescopes remain vulnerable to a variety of air- and space-borne transmitters. Due to the altitude and growing density of satellites, especially those found in large satellite constellations, their transmissions are becoming a constant presence and are increasingly difficult to avoid via simple scheduling by radio telescopes, even if sited in the most remote regions of the Earth. As a result of this development, a number of radio astronomy sites have implemented a system called Operational Data Sharing (ODS) to facilitate information sharing with satellite operators.

The simple goal of ODS is to make the near real-time activity of the radio telescope (sky position, frequency, bandwidth) available to a satellite operator. Based on this information, the satellite operator sends commands to particular satellites that cause e.g. to change their behaviour in such a way as to minimize downlink signal strength for the short period of time when the satellite is close to boresight of a radio telescope (typically on timescales of seconds). In practice, an operator typically requires at least 10 to 20 min lead time to effect mitigating changes on their system, in some cases several hours. Reverse information sharing from the satellite operator with the radio observatory is also envisioned under this framework, e.g. providing metadata on actions taken. As a reporting schema, the usefulness of ODS and ODS-like systems is not necessarily limited to space-based transmitters.

Since the initial testing, the ODS system has been considered for use beyond U.S. National Radio Astronomy Observatory instruments, such as the Hat Creek Radio Observatory, MIT Haystack Observatory, SKAO, and CSIRO instruments. An example data format developed for this purpose is provided in Annex 1.

4.4.1 Boresight avoidance technique

One of the mitigation techniques employing coordination with active users, which has been implemented in the real-world is the so-called "telescope boresight avoidance". This technique

enables satellites to avoid transmissions into the line-of-sight of radio telescopes by leveraging phased array antenna technology, which can dynamically steer satellite beams away from telescopes (outer boresight avoidance) in milliseconds or briefly cease transmissions (inner boresight avoidance). This technique leverages the ODS system for near real-time data exchange, as described in the previous section.

To implement such systems the following steps have shown to be beneficial:

– Typical boresight avoidance parameters are determined from simulations using idealized antenna patterns and are used for initial implementation.

– To verify and test the success of applying boresight avoidance and to refine telescope specific parameters, coordinated testing between the observatory and satellite operator is required. The satellite operator would be expected to provide ephemerides for its satellites, and predicted close passes to a given telescope pointing direction. The telescope operator observes at the agreed-upon pointing direction, in a band where they expect to see interference from the satellite system. During the test, the satellite constellation operates normally for half of the test duration, then enables boresight avoidance on half of its downlink channels during the other half of the test. Once the telescope has the data from its observations, the received signal levels are compared with and without boresight avoidance enabled, and determine whether interference attributable to the satellite systems' beams was effectively reduced to the required levels. If not, the satellite operator adjusts boresight avoidance parameters based on the observed data, and the testing process is repeated as needed, until the appropriate boresight avoidance parameters are determined. A description of a first successful demonstration of boresight avoidance is provided in Annex 1.

– Once testing is complete, radio observatories set up an ODS system to provide data on a telescope's upcoming observations (time, pointing direction, and band observed). The satellite operator will then automatically fetch this data from the observatory and apply boresight avoidance with the parameters determined from the coordinated testing.

While this combination of a ODS system with application of telescope boresight avoidance has been largely successful, there are still challenges that this solution will not fully address, including: (1) Boresight avoidance is unlikely to prevent all signals from entering the beam due to sidelobes, scatter, etc.; and (2) systems like this might present challenges in terms of implementation due to a variety of factors (satellite systems unable to respond, or unable to respond quickly to the requests; the need for telescopes to respond scientifically to the weather, scientific finds, etc.) (3) Studies have shown that boresight avoidance alone under certain assumptions reduces the epfd by about 10 dB only. Furthermore, these methods are not yet proven effective in all interference scenarios (e.g. aggregate sidelobe interference, dynamic scheduling, intermodulation) and is likely to put burden on radio telescope operators in managing a real time radio telescope antenna pointing direction database that is not always feasible (e.g. target-of-opportunity observations). If considered, this technique should be considered supplementary and not used to comply with the single-entry 2% criteria of the radio astronomy service (Recommendation ITU-R RA.1513).

5 Spatial excision (nulling)

5.1 Multi-antenna systems

Every multiple-antenna array has sidelobes and nulls in its beam pattern that can be used to reduce signals from localized sources of RFI. Manipulation of the antenna outputs may create a spatial response null in the direction of incident RFI [83]. Such methods as a group are known variously as adaptive array processing, adaptive beamforming, statistically optimal beamforming, or adaptive

cancelling. A variety of specific algorithms including maximum SNR, linearly constrained minimum variance (LCMV), subspace projection, Wiener filtering, and multiple sidelobe cancelling [82], [83] have been studied by a number of researchers for application to radio astronomical observing ([11], [12], [13], [23], [27], [40], [43], [54], [57], [58], [61], [70], [81]).

In general, an adaptive system using a beam-forming algorithm requires a high INR and is limited to a small number of RFI targets to be tracked during an observation. The RFI sources also need to remain stable and predictable through an observation. Spatial filtering in beam-forming mode for a limited number of RFI sources generally does not degrade the image generated by the main beam.

The basic technique is well known from its applications in military "anti-jam" communications as well as commercial cellular telecommunications applications [59]. In principle, the same techniques are applicable to radio astronomy. In practice, however, there are complicating factors. First is the fact that in radio astronomy, unlike traditional commercial and military applications, RFI is damaging even when the INR << 1. Thus, to be effective, null-forming algorithms must successfully detect and localize RFI at these levels. In contrast, RFI in commercial and military applications is typically not problematic until the INR is ~1. For this reason, most null-forming algorithms developed in the context of military and commercial applications are based on the Wiener filter strategy (which includes so-called "power minimization" and "minimum variance" algorithms), which perform poorly for INR < 1 [27].

It is known that techniques based on Wiener filtering are limited to reducing the INR in proportion to the INR; i.e. it is straightforward to suppress RFI to a level of an INR ~ 1, and relatively difficult to reduce it further. Thus, to make such techniques effective for radio astronomy, additional measures are typically required to increase the apparent INR delivered to the mitigation algorithm; a few of these are discussed below. It is possible to improve nulling performance if auxiliary antenna signals are available to provide a direct look at the interferer with a higher INR [16] [43].

Radio astronomical observations depend upon the antenna performance (e.g. gain, beam profile, side-lobe distribution). Traditionally, this has been achieved by precise measurement and attention to ensuring that these parameters do not change with time. Variations in the sidelobe pattern may confound the self-calibration algorithms used to produce high-dynamic range images in aperture synthesis interferometry. Maintaining or at least knowing the variation in these parameters as the antenna beam and sidelobe pattern are modulated in order to mitigate interference is a challenge for the signal processing and antenna control systems now in widespread use.

5.2 Subspace projections

An alternative to traditional Wiener filter-based null-forming techniques is the class of techniques based on "subspace projections". The basic idea in subspace projection is that interference can be identified in terms of correlations between the array elements, which in turn can be used to determine beamforming coefficients that result in patterns which reject the interference with little or no effect on the main lobe characteristics. In mathematical terms, subspace projection is a two-step process of:

– identifying the eigenvectors of the spatial covariance matrix (the set of pair-wise correlations between elements) followed by;

– making the vector of beam forming coefficients orthogonal (the "projection" operation) to the eigenvector associated with the interference (the interference "subspace").

Normally, it is assumed that the interference dominates the power received by the array, so that the interference subspace is always the one associated with the largest eigenvalue of the spatial covariance. This leads to problems when the interference is relatively weak, especially if the INR < 1 [27]. Nevertheless, subspace projection has been shown to have significant advantages for radio astronomy when properly employed [70]. Such techniques are not a panacea for the problem of poor

detection and localization performance, but they do offer reduced distortion of the antenna pattern and, to some extent, behaviour that is easier to anticipate and modify. Distortion introduced by this class of techniques can even be corrected in aperture synthesis imaging as a post-processing operation [58]. A method to eliminate beampattern distortion in power spectral density estimation, while nulling a moving interference source, has also been demonstrated [45]. Another type of bias distortion caused by nulling beamformers when the interferer is narrowband has recently been identified [46].

Even though the null is intended to attenuate only signals from a single direction, the temporal spectrum of the SOI is "notched out" at the same frequency as the interferer using an algorithmic solution. It has recently been shown that if sufficient computational resources are available to store and process a several seconds window of data, much deeper nulls can be formed, even with rapidly moving interference, by fitting the time-varying interference covariance structure to a matrix polynomial model [55].

In general, null-forming is most applicable to mitigation of RFI from satellites, and can be expected to be somewhat less effective against terrestrial RFI. This is because terrestrial RFI is often scattered by intervening terrain, and often arrives at the radio telescope as a dynamically-varying and complex wave front with apparent direction of incidence spread out over a significant angular range. Traditional null-forming techniques are typically degraded in the presence of angle spread, and the problem gets worse with decreasing INR.

5.3 Post-correlation beamforming

An alternative to the implementation of spatial nulling in real time is to implement "post-correlation" beamforming. Particularly for sparse arrays, with relatively long baselines, correlation may be performed first and the beams synthesized afterwards. "Correlation" in this sense refers to the cross-multiplication of independent antenna outputs (e.g. polarizations, or separate antennas in an array), followed by averaging of the spectrum of the products. It is common for single dish radio telescopes to correlate to obtain Stokes parameters and for arrays of dishes to cross-correlate dishes as a step in synthesizing images. The same beamforming weights, which are used with the time series samples of the array output to form the beam, can instead be applied directly to the integrated correlations to obtain an effective total-power-per-beam-per-frequency-channel spectrometer result that is identical to an integrating spectrometer applied to the time series output of the adaptive beamformer. Assuming the RFI sources are localized, their suppression with this method is then achieved by processing short time intervals of the data stream, and applying complex weighting during image processing [41]. Computer simulations of post-correlation spatial filtering show that cleaning with an RFI-corrected beam can be effective [57]. Also included in this category are aperture synthesis imaging techniques, which exploit the correlation products already available to similar ends (see [20] for a recent example).

This method is effective in total power or spectrometer observations, but not for time sequence dependent applications such as pulsar processing. It has the advantages that the same correlation computations can be used both to calculate the beamforming weights and then to compute the corresponding beamformer output power for those weights. This can all be done after the fact in post processing using stored, integrated correlations.

5.4 Reference antennas and reference beams

Auxiliary reference antennas can be cross-correlated with the primary antennas. As long as the auxiliary antennas receive the desired astronomical signals with very low SNR and the RFI signals to similar sensitivity, it is a simple matter to correct the RFI-corrupted correlation products using the hybrid (telescope output correlated with auxiliary antenna) correlation products. The technique was first described by Briggs *et al*. [16], and was later shown to be essentially equivalent to time-domain

("pre-correlation") cancellation, with the exception that additional INR is obtained with no special effort through the integration of the correlation products.

Successful experiments using this approach have been done using one of the 14 antennas of the Westerbork Synthesis Radio Telescope as a reference antenna [37]. This technique shows great promise for the emerging generation of radio telescope arrays, for which it should be possible to synthesize high-gain auxiliary beams from the same antennas, as opposed to requiring additional "physical" antenna elements.

Correlators for modern radio telescopes are extraordinarily complex and expensive systems. So, this approach requires a significant increase in the capacity of the correlator in order to compute the required additional correlation products and apply them to achieve RFI cancellation. Furthermore, the dynamic nature of most RFI signals limits the amount of integration that can be applied for effective use of this technique: "dump times" on the order of tens of ms may be required to mitigate satellite signals or signals which experience multi-path fading. The necessary increase in the capacity of correlators combined with reduced dump times may increase cost and complexity beyond practical limits, and the increased degree of data processing will result in some degree of data degradation.

Smart antenna techniques, using multiple sensors in radar and communication systems, are used to determine the direction-of-arrival and to implement beam-forming algorithms. Similarly, multiple-sensor, new-generation telescopes with a direct view of identified RFI sources (such as LOFAR and the Murchison Widefield Array) allow the beam-forming process to be optimized to include real-time, adaptive nulling and spatial filtering of these distinct RFI sources [80] [14]. In a practical implementation, one hundred LOFAR antennas were used to generate two separate beams, while placing a permanent null at one position 15 degrees above the horizon [58]. Well-calibrated, multi-sensor, phased arrays offer the possibility of steering a null to track a satellite, while maintaining a high-gain beam on a target field [34]. However, the processing complexity increases rapidly when coping with a multi-satellite system.

Focal plane array (FPA) systems and multi-beam receivers provide new opportunities for spatial filtering, as each of the component feeds has an independent sky signal together with the common RFI signal [12] [40] [52]. In addition, one of the feeds in a multi-beam system can always be used as a reference antenna.

Overall, spatial nulling techniques remain largely untested due to their high complexity and the large engineering costs associated with development and implementation. Even in the most favourable situations, the data obtained will not be of the quality that would have been the case in the absence of interference.

6 Waveform subtraction

As adaptive noise cancellation (ANC) is often used in both communications and military technology, there is a considerable body of experience in the use of waveform subtraction algorithms [42]. The basic principle of temporal adaptive filtering is to make a FFT from the incoming data, perform an adaptation operation on the frequency bins, and then return to the frequency domain via an inverse FFT. This method, based on Wiener filtering, works for interfering signals with a significant INR, i.e. when the RFI dominates the system noise. The suppression of the interfering signal can be about equal to its instantaneous INR. Adaptive filters are effective when spectral information is unimportant, such as in pulsar [50] and continuum studies. An equivalent process can also be implemented in the frequency domain.

An optimal single-dish temporal cancellation algorithm involves the following steps:

Step 1: Detection and estimation of the RFI waveform.

Step 2: Synthesis of a noise-free version of the RFI waveform.

Step 3: Subtraction of the synthesized RFI waveform from the afflicted data.

This strategy was investigated first in the context of radio astronomy by Barnbaum and Bradley [6], who used a "least mean squares" (LMS) algorithm with a technique based on Wiener filter principles. But the applicability of this technology to radio astronomy is limited by the need for an input INR > 1 in order to achieve significant benefit. To achieve an output INR << 1 using this method, it is usually necessary to implement some means to receive the RFI with an INR greater than the INR perceived by the primary instrument. One way to achieve this is to use a separate directional antenna to receive the RFI [6]. Since most large dishes have a sidelobe gain that is approximately isotropic in the far sidelobes, the INR can be improved approximately in proportion to the forward gain of the auxiliary antenna used to receive the RFI. Thus, for example, a yagi with a 20 dB gain could improve the INR available to the cancellation algorithm by about 20 dB, which could then reduce INR at the telescope output by a comparable factor. Subsequent work [43] describes the extension of this "reference signal" approach to achieve better performance against RFI from satellites by using multiple auxiliary signals from dishes with gains on the order of 30 dB.

Another perspective on this performance issue from a more theoretical viewpoint is provided by [22], who found that the suppression achieved by a cancellation algorithm is approximately upper bounded by the product of the input INR and L, the number of samples used to estimate the waveform parameters, assuming a noise bandwidth equal to the Nyquist bandwidth, and is otherwise scaled by the ratio of the noise bandwidth to the Nyquist bandwidth. So, for example, to suppress a signal with INR equal to −20 dB by an additional 20 dB requires analysis of at least 10 000 Nyquist-rate samples, and proportionally more if the noise bandwidth is less than the Nyquist rate. Of course, the signal characteristics must also be stationary over this timeframe, so this can easily become the limiting factor.

A limitation of cancellation techniques that employ auxiliary antennas to obtain a reference signal with high INR is that such techniques can easily degrade into excision. For example, a single-dish radio telescope combined with a high gain auxiliary antenna can behave as a two-element array, with the result that the cancellation algorithm may synthesize a pattern null in the direction of the RFI, with the same consequences as those described above that are associated with null-forming. Yet another consideration is that it is a potentially onerous task to localize and point reference antennas for every source of RFI that affects an observation.

An alternative temporal cancellation approach that avoids these difficulties is to synthesize distinct reference signals directly from the telescope output itself, by exploiting *a priori* knowledge of the modulation characteristics. For example, Ellingson *et al*. [25] demonstrated a technique for mitigation of RFI from a GLONASS satellite by partially demodulating the signal and then re-modulating the result to obtain a noise-free estimate of the RFI. They demonstrated a reduction of the INR by more than 20 dB despite the fact that the RFI was received with INR on the order of −20 dB. In this case, the INR "deficit" was overcome by the effective increase in INR associated with the process of demodulation. It should be noted that this same technique could also be used to further improve the INR obtained by using auxiliary antennas.

Unfortunately, signal modulations of the type used by GLONASS (i.e. direct sequence spread spectrum) represent only the "low hanging fruit" with respect to one's ability to obtain large INR improvements through partial demodulation. Most other signals do not exhibit such large improvements with similar processing, and less can be done if the modulation is analogue or has unknown structure. For example, work by (Roshi, 2002) on a similar strategy for analogue TV signals

achieved only about 12 dB suppression despite beginning with an initially large INR, and work by Ellingson and Hampson [27] demonstrated suppression on the order of 16 dB against radar pulses using an estimate-synthesize-subtract strategy. A recent implementation of adaptive filtering techniques aims to remove the signature of the L3 transmission from a single GPS satellite at the Arecibo Observatory [63].

This cancellation methodology has also been used effectively with multi-feed or focal plane arrays on single dishes. A variation on adaptive filtering is to subtract a reference data-channel from a signal data-channel using a copy of the RFI itself, by comparing on-source plus RFI and off-source plus RFI signals.

In summary, while nominally more desirable than excision, temporal cancellation involves a significant risk that the waveform is not properly estimated, and therefore not completely removed when the synthesized waveform is subtracted. Whereas the performance of excision is limited primarily by one's ability to detect RFI, the performance of cancellation is limited primarily by one's ability to estimate the RFI waveform. The price paid for the benefit of the "look through" capability offered by cancellation is performance that is potentially limited and less-robust than comparable excision techniques. Yet, innovative and useful work continues in this area: the productive use of adaptive cancellation has been demonstrated in pulsar astronomy [50], and the use of real-time hardware has been demonstrated for implementing adaptive cancellation [68].

The ability to cancel interference by waveform subtraction is limited by the quality of the cancellation waveform as an estimate of the interference waveform received by the radio telescope. Any shortcoming in this estimation process results in some degree of data degradation.

7 Anti-coincidence methods

Instead of mitigating RFI, anti-coincidence techniques detect its presence in data. These techniques exploit the fact that widely-separated antennas perceive astronomical signals identically, but RFI differently. The primary use of this technique is in searches for astronomical transients, which are otherwise severely limited in practice by impulsive RFI. Depending on the range of the interfering signals, separations on the order of hundreds of kilometres may be required: this is of course an awkward strategy to use, except in the rare cases where similar telescopes are suitably separated while sharing the same field of view. Cancellation cannot be perfect, and residual random fluctuations do result in data degradation. Nevertheless, this technique has been successfully applied to all-sky transient searches [48] and to searches for one-time "giant" pulses from pulsars [10].

8 Temporal and frequency data flagging

8.1 Temporal blanking

Temporal blanking is perhaps the oldest and best-known strategy for real-time mitigation of pulsed RFI, and has been used as a response to ground-based aviation radars operating in the 1 215-1 400 MHz band. These typically transmit pulsed fixed-frequency or chirped sinusoidal waveforms with pulse lengths of 2-400 μs with 1-27 ms between transmitted pulses and bandwidths on the order of 1 MHz.

These pulses are often detectable through the sidelobes of radio telescopes situated hundreds of kilometres away. Although the transmission duty cycle is relatively low (typically less than 0.1%), accurate blanking is made difficult by the short interval between pulses, as well as by multi-path reflections from terrain features and aircraft generate additional copies of the pulse, which arrive long after the "direct path" pulse (see, e.g. appendix of [28]). It is common for multi-path pulses to be

strong enough to corrupt the astronomical observations even though they are too weak to be detected reliably. Thus, a blanking interval triggered by a detected pulse must typically be many times longer than the detected pulse, in order to ensure that all of the multi-path copies are blanked. Blanking intervals with lengths up to 100's of microseconds (i.e. 10-100 times the pulse duration) are typically required [28].

A number of real-time techniques for temporal blanking or cessation of the data-taking process have been developed to various degrees [32] [85] [58]. The National Astronomy and Ionosphere Center (NAIC) has developed a device for real-time mitigation of strong pulses from the local airport radar at the Arecibo Observatory (Puerto Rico). This works by tracking the arrival time of the leading edge of the pulses, and then blanking the output of the receiver in a time window around the expected pulse arrival times. tailored to encompass the consequent radar artifacts from terrain and multi-path scattering. More recent work in this area, including experimental results, is described in Ellingson and Hampson [28], Fisher *et al.* [31], and Zheng *et al*. [88], with the last two references addressing the similar problem of pulsed interference from aviation distance measuring equipment (DME).

The primary limitation for the blanking approach is detection performance, since an RFI pulse is detected, it can be completely removed by blanking. However, it is inevitable that some fraction of weak pulses will not be detected. Over the time-scale of a single pulse, however, astronomical signals routinely have a signal-to-noise ratio (SNR) $<<1$, so RFI must be reliably detected at these levels in order to be effectively suppressed in the integrated output.

This is quite difficult: the recent successes cited above are attributable to detailed advanced knowledge of the RFI waveform, which is used to compensate for an inadequate SNR in detecting the radar pulses.

Further improvements in detection performance appear to be feasible using aspects of the RFI waveform that can be exploited without specific knowledge of the waveform. Thus cyclo-stationarity has been applied by Britteil and Weber (2005) [17] to the HIBLEO2 (Iridium) Satellite signals, while Dong *et al.* [22], have applied Kalman tracking to aviation radar, which also improves detection performance at lower interference to noise ratios (INR). Another challenging problem is presented in determining exactly how to set detection thresholds and blanking window lengths so as to achieve an acceptable trade-off between robust RFI mitigation (which suggests low thresholds and long windows) and limiting degradation of sensitivity and the introduction of blanking artifacts (which suggests high thresholds and short windows). This problem was studied by Niamsuwan *et al*. [62]. Nevertheless, "blanked" time is lost observing time that requires an increase in the observational time to achieve the desired sensitivity. Additionally, any remnant signal from the RFI can readily result in false or incorrect detections for the scientific data, making the results unreliable.

8.2 Antenna-based digital processing

Real-time digital processing may be implemented as part of the signal chain of a single-dish radio telescope (RT), and as part of the station processing and/or beamforming process for array instruments. This cost-effective method works well for impulsive (transient) RFI and requires fast data sampling as well as the availability of sufficient computing cycles at each of the stations [37] [62] [28]. The amount of data loss is determined by the transient nature of the RFI. Real-time, IF-based flagging and excising minimizes the data loss incurred by the flagging – excision method by only dealing with the RFI-infected time and frequency segments; this should not inflict collateral damage on neighbouring time and frequency intervals. This differs from post-correlation processing (next section), which is more vigorous as integrated data samples are used for baseline and antenna flagging and excising. Thresholding in both the temporal and frequency domains may be applied when the RFI in sampled data is strong and identifiable, and the spectral occupancy of the RFI is relatively low. Thresholding was first used to remove RFI at the Ratan 600 m telescope [9]. A recent

application was at the Westerbork Synthesis Radio Telescope (WSRT), where 20 MHz dual-polarization IF data from each of the fourteen telescopes was processed in real-time [3] [4]. This thresholding method has also been applied to pulsar data prior to period folding [35] [36].

Another form of sub-space excision exploits the probability distribution analysis of signals. Since the RFI contribution changes the power spectrum to a non-central (chi-square) distribution, as determined by its higher moments, it can be removed from data [37] [33]. A similar approach exploits kurtosis (4^{th} moment of the power spectrum) to identify and remove the RFI component. Kurtosis has been used as the RFI discriminant for single-dish real-time solar observations by Nita *et al*. [64], Gary *et al*. [39], and by Deller [21] for post correlation processing in a software correlation environment. Median filtering and taking advantage of the median properties of a multi-feed system, also exploit the statistical properties of data and are effective in the real-time mitigation of RFI in spectral-line data [47] [38].

Pre-correlation mitigation methods that involve the removal of data samples necessarily change the gain calibration of data. So, the use of these methods requires accurate bookkeeping to determine their effect on data and associated data loss. On the other hand, replacing affected data in the frequency (or time) domain with a fitted baseline only affects the rms of affected channels, although here this replacement could affect the perceived strength of the astronomical signal, if it lies within the affected channels.

This kind of data blanking has been implemented in production for the Karl G. Jansky Very Large Array (VLA) Wideband Interferometric Digital Architecture (WIDAR) correlator. The WIDAR Station Boards provide a capability to excise or "blank" impulsive radio frequency interference on microsecond timescales, thus avoiding the corruption of the longer visibility integrations that are typically accumulated over a few seconds. This mode is particularly effective at identifying and blanking interference from radar transponders, especially those used for aeronautical navigation between 1.0 and 1.2 GHz. The blanking applies to the voltage sample time-series recorded for each subband on a per station (i.e. antenna) basis before cross-correlation. The voltage samples are recorded at 256 megasamples per second (~4 ns) and sample values that exceed a dynamically set threshold are flagged as bad data for a fixed dwell time and ignored. Thus, by blanking in time, the whole subband is effectively blanked in frequency. Typical fractions of blanked data are approximately 0.1% of data per integration per subband.

These techniques have proven to work well within limited cases, and research is still underway to increase the opportunities for pre-correlation mitigation.

8.3 Digital excision at correlation

As part of the correlation process, digitized data are generally integrated over time intervals ranging from the sampling time up to seconds, which significantly raises the INR. In consequence, persistent but weak RFI, that could not be treated in real-time, and weak (spectral) remnants of earlier mitigation operations become accessible for processing. On the other hand, significant peaks of a time-varying RFI signal may also be reduced in strength by the integration process. For array instruments, spatial filtering resulting from delay (fringe) tracking of a celestial source also reduces the strength of terrestrial RFI in cross-correlated data.

At this point in the data taking process, anti-coincidence protocols may be incorporated to identify the RFI components, as well as digital mitigation processing and the utilization of data from a reference antenna. New generation software correlators permit the integration of kurtosis-based flagging applications before and after FX (Fourier Transform before multiplication) correlation and stacking protocols [21]. Mitigation at several processing stages is being implemented for LOFAR [8].

In the case of single-dish instruments the correlation processing of (multiple) single bands may incorporate both thresholding or statistical methods and noise cancellation with a reference antenna.

Subspace filtering methods may also be implemented in a digital correlation system to search for a particular signature in the RFI power component of data in order to identify and remove it. A particularly successful application is the search for cyclo-stationarity within data, which works well for digitally modulated RFI signals [86] [29] [30].

Deploying digital processing and input from reference antennas during software correlation is equivalent to their use in baseband pre-correlation processing. But the implementation of these algorithms into pre-existing hardware backends requires the addition of both special hardware and software. As with the pre-correlation excision techniques, this method remains limited as there is still considerable research to improve and generalize the algorithms, thereby increasing the variety of RFI on which the technique can be accurately used, and decreasing any remnant signal from the RFI.

8.4 Post-correlation – Before or during imaging

Traditional post-correlation processing consists of flagging and excising, which is time consuming and often done at least partially manually [56]. Because this operation is performed on integrated and correlated data, the data loss resulting from flagging can be quite significant, the more so as whole time-slots, whole baselines, and/or whole antennas may be flagged. This differs from antenna-based signal-chain flagging or excising where small subsets are flagged, which inherently results in a smaller proportion of data loss overall.

On-line or off-line processing of (integrated) correlated data makes it possible to incorporate automated flagging and excision ([60] [66] [67] [49] [75] [76]), as more sophisticated statistical or sub-space processing (see § 8.2) can be implemented to remove the RFI component without as much data loss. There are many techniques in use for post-correlation mitigation of RFI signals, and the choice of technique to use is dependent primarily on the type(s) and density of RFI present, hardware used for the observations, and the scientific goal of the data set.

Briggs *et al.* [16] implemented a reference antenna at the post-correlation stage to remove the signal from a well-defined RFI source using the available closure relations.

Array instruments employ fringe-stopping and delay-compensation techniques to keep a zero-fringe rate at the central observing position during observations. As a result, the stationary (terrestrial) and satellite RFI components in data distinguish themselves by fringing faster than components from astronomical sources. This distinctive (relative) motion allows the off-line identification and elimination of stationary RFI sources from both the correlated data and the image plane without causing data loss [87] [20] [1]). The coding for this operation from the GMRT is now incorporated into AIPS [53].

Another emerging and powerful method are algorithms that perform RFI flagging in the Fourier domain. For example, one can take advantage of redundancy of complex visibilities inside the Fourier image plane to identify corrupted data or use a scheme to detect faint RFI in the complex visibility time-channel plane of individual baselines [74].

9 Implementation at the telescopes – A strategy

The data acquisition process of radio astronomy observatories is evolving to cope with the rapidly changing technological environment. Analogue to digital conversion of signals now occurs as early as possible in the data-handling scheme, which allows digital processing throughout most of the data chain. Increased instrumental capabilities allows for the processing of larger bandwidth data, with higher time-resolution and higher frequency (< kHz) resolution.

Many current signal processing systems do not allow the implementation of mitigation at early stages of the data handling chain without incurring (severe) hardware modifications. By contrast, new-generation backends and software correlation facilitate such schemes at different stages of the processing.

Since every mitigation method requires a definite INR threshold for its operation, removal of most of the RFI requires a layered application of methods to exploit the progressive integration of the data and its increasing INR. While no method can remove RFI below the noise floor it encounters, subsequent mitigation steps may remove remnants of the mitigated RFI, as well as weak RFI that is only apparent after integration.

The implementation of auxiliary antennas for array instruments depends on the possibility of incorporating their output into the processing system (most particularly) at the correlator. Directed reference antennas generally cope with particular RFI sources and are less effective in a complicated environment.

Human intervention in the RFI mitigation process currently plays an important role in practical operations. Thus real-time on-line processing that is adaptable to a variety of RFI signatures may be preferred to the restrictive use of reference antennas and/or spatial filtering for known and fixed transmitters. This is likely to be the case until an artificial intelligence controller can be invoked to guide and dictate the RFI mitigation scheme.

Interferometers are less vulnerable to RFI. Fringe-stopping and de-correlation by delay compensation provide for its natural suppression on the longer baselines. However, strong RFI still adds to the system noise, and still affects the calibration and the complex visibilities of a station. VLBI stations and distributed sensor networks can implement mitigation at every individual station to reduce the impact of local RFI on the whole system.

To correctly calibrate a system, accurate bookkeeping is required for all affected data in order to obtain the correct weights for later self-calibration, cleaning and imaging procedures.

Future mitigation implementations need to consider more sophisticated methods than the simple (kurtosis or other) RFI flagging and excising algorithms that are generally current at this time. The use of statistical methods using higher moments opens the possibility of removing RFI components without affecting the rest of the data, and there are methods that allow partial restoration of data that reduce data loss. Adaptive filtering of spread-spectrum systems may become possible when their digital keying schemes are known. In all cases, though, care must be taken to ensure integrity of the scientific signal, and it should be recognized that RFI flagging or excision remains a poor substitute for mitigation in advance of the observations being taken, regardless of where in the signal chain the excision occurs.

10 Summary

RFI mitigation technology and techniques offer significant benefits to radio astronomy, but more work remains to develop technology that is practical and applicable in routine operations and which ensures the integrity of the scientific data obtained. It is also clear that RFI mitigation technology cannot be regarded as a standalone fix for the external RFI problems experienced by present day and future radio telescopes. Inevitably, the effectiveness of any given technique depends on:

– the architecture of the instrument or its configuration for a particular observation;
– the observing mode and scientific goals (e.g. spectroscopy, continuum, aperture synthesis imaging, pulsar dispersion searching);
– the nature of the RFI itself (e.g. persistent or intermittent, spatially coherent or scattered by multi-path);

– availability of resources needed to implement computationally intensive algorithms, when required;

impact on the flexibility of the astronomical observations that could be accepted;

– the accuracy of the results and subsequent comfort level of astronomers to use these new techniques and instruments.

Mitigation merely reduces the degree to which data are degraded or obliterated by interference, it does not remove all traces of RFI from the data without effect. Additionally, mitigation increases operational costs. As an example, if RFI is merely flagged from the data, the overall measurement time to reach the target sensitivity is increased. The near-term path to bring RFI mitigation into practical use is for researchers in signal processing to work together with astronomers to identify specific, high-value science observations which currently cannot be undertaken due to RFI, for which mitigation algorithms can be applied and tested. It should be noted, however, that no, single technique can address all possible scenarios for radio astronomy observations, nor is one thought to be possible. Mitigations that take advantage of high-speed information sharing between active and passive users of the spectrum hold promise and should be further investigated.

Both on-line and off-line data processing has been successful in mitigating the RFI environment of radio astronomy observatories. While there is an increasing variety of successful mitigation options, the choice of method depends strongly on the RFI characteristics, the type of radio telescope, and the type of observation. In particular, on-line real-time data-processing may be preferred in a variable RFI environment, while special measures such as reference antennas and spatial filtering may be preferred for known and fixed sources of RFI. In addition to these factors, the absence of human involvement may also render automated on-line processing a more attractive option.

No universal method exists for mitigating RFI in astronomical data and no method can identify or remove RFI within the noise of the system. The effective suppression of RFI depends on the INR and its temporal and spectral characteristics. A quantitative evaluation of the method used is not always possible because mitigation algorithms are generally non-linear processes that also affect the noise characteristics and the gain calibration. The toxicity of the method used, i.e. the negative effect of its invocation on data by the deployed method, and the amount of data loss resulting from the method, are other factors that guide the evaluation of the choice of method.

Multiple methods need to be applied to deal with a more general RFI environment. Because RFI characteristics change after each mitigation step and with increasing integration of the data, the cumulative effect of RFI mitigation at subsequent stages is not a linear sum of what each method can do, but rather the sum of what is practical and possible at each step.

The cost of computing hardware capability and of digitizing components at radio astronomy observatories is rapidly changing. Both upgrades of existing facilities and the introduction of newly constructed instruments provide opportunities for implementing and automating RFI mitigation algorithms. These capabilities also permit increased bandwidth, higher time resolution, and higher spectral resolution. The resulting, increasingly large data volumes will force the introduction of automated data reduction pipelines. Future data volumes are likely to force the acceptance of automated RFI mitigation at radio observatories.

New telecommunication and broadcasting technologies are reaching the marketplace, many in the form of unlicensed mobile devices. Since their ever-changing locations are impossible to control, they will rapidly affect observatory operations. Algorithmic research is needed to eliminate their signals from astronomical data. In particular, spread spectrum (ultra-wide band) devices will pose problems for passive services, as their digital modulation schemes do not respect the boundaries of spectrum allocations. Current estimates suggest that the number of transmitting devices used by each person is set to increase dramatically and many of these will rely on dynamic spectrum access.

The discovery space for radio astronomy is determined to a significant degree by the technical characteristics of the observing system and by limiting factors such as the RFI environment. While new generation telescopes are located at the most pristine possible sites, existing facilities must coexist with their local conditions. In order to prevent RFI becoming the limiting factor for existing facilities, spectrum management, both internal and external, has to be accorded a very high priority. Both observatory management and astronomers should regard RFI issues as critical.

References

ITU-R References

Recommendation ITU-R RA.769 (2003), *Protection criteria used for radio astronomical measurements*, International Telecommunication Union, Geneva, Switzerland.

Recommendation ITU-R RA.1513 (2003), *Levels of data loss to radio astronomy observations and percentage-of-time criteria resulting from degradation by interference for frequency bands allocated to the radio astronomy on a primary basis*, International telecommunication Union, Geneva, Switzerland.

ITU-R Handbook (2003), *Handbook on Radio Astronomy, International Telecommunication Union*, Geneva, Switzerland.

Academic References

[1] ATHREYA, R. (2009), *A New Approach to Mitigation of Radio Frequency Interference in Interferometric Data*, ApJ 696, 885.

[2] BAAN, W.A. & BOONSTRA, A.-J., 29-31 March, 2010, Groningen, The Netherlands.

[3] BAAN, W.A., FRIDMAN, P.A. and MILLENAAR, R.P. (2004), *Radio frequency interference mitigation at the Westerbork Synthesis Radio Telescope: algorithms, test observations, and system implementation*, AJ 128, 933.

[4] BAAN, W.A., FRIDMAN, P.A., MILLENAAR, R.P. and ROY, S. (2010), *The WSRT Interference Mitigation System – lessons learned*, PoS (RFI2010) 024.

[5] BAAN, W.A. (2010), *Setting the stage – layers of RFI Mitigation, RFI2010 – RFI Mitigation Workshop*, PoS (RFI2010) 001.

[6] BARNBAUM, C. and BRADLEY, R.F. (1998), *A new approach to interference excision in radio astronomy: real-time adaptive cancellation*, Astronomical Journal, 116, 2598.

[7] BELL, J.F., EKERS, R.D. and BUNTON, J.D. (2000), *Summary of the Elizabeth and Frederick White Conference on radio frequency interference mitigation strategies, Publications of the Astronomical Society of Australia*, 3, 17.

[8] BENTUM, M., BOONSTRA, A-J., MILLENAAR, R.P. and GUNST, A. (2008), *Implementation of LOFAR RFI mitigation strategy, Proc.XX1X GA (URSI Chicago)*, 348, 2008. http://scholar.google.com/citations?view_op=view_citation&hl=en&user=7mLAYBAAAAAJ&citation_for_view=7mLAYBAAAAAJ:W7OEmFMy1HYC

[9] BERLIN, A.B. and FRIDMAN P. (1996), *Real-Time Radiometric Data Processing against Electromagnetic Pollution*, Proc. XXV URSI GA (URSI Gent), 750, 1996.

[10] BHAT, N.D.R., CORDES, J.M., CHATTERJEE, S. and LAZIO, T.J.W. (2005), *Radio frequency interference identification and mitigation using simultaneous dual frequency observations,* Radio Sci., Vol. 40, 5, RS5S14.

[11] BOONSTRA, A.J. (2005), *Radio Frequency Interference Mitigation in Radio Astronomy, Ph.D. Dissertation*, Technical University of Delft, The Netherlands.

[12] BOONSTRA, A.J. and VAN DER TOL, S. (2005), *Spatial filtering of interfering signals at the initial low frequency array (LOFAR) phased array test station. Radio Sci.*, Vol. 40, 5, RS5S09.

[13] BOWER, G.C. (2005), *Radio frequency interference mitigation for detection of extended sources with an interferometer, Radio Science*, Vol. 40, 5, RS5507.

[14] BREGMAN, J.D. (2000), *Concept design for a low-frequency array*, Proc. SPIE, 4015, 19.

[15] BRIGGS, F.H. and KOCZ, J. (2005), *Overview of Technical Approaches to Radio Frequency Mitigation, Radio Science*, Vol. 40, 5, RS5S02.

[16] BRIGGS, F.H., BELL, J.F. and KESTEVEN, M.J. (2000), *Removing radio frequency interference from contaminated astronomical spectra using an independent reference signal and closure relations*. Astronomical Journal, 120, 3351.

[17] BRITTEIL, S. and WEBER, R. (2005), *Comparison of two cyclostationary detectors for radio astronomy interference mitigation in radio astronomy*, Radio Sci., Vol. 40, 5, RS5S15.

[18] CLERC, V., WEBER, R., DENIS, L. and ROSOLEN, C. (2002), *High Performance Receiver for RFI Mitigation in Radio Astronomy: Application at Decameter Wavelengths*, EUSPICO'02, Toulouse, France.

[19] COHEN, J., SPOELSTRA, T., AMBROSINI, R. and VAN DIEL, W. (2005), *CRAF Handbook for Radio Astronomy (Third Edition)*, European Science Foundation, Strasbourg, France. http://www.craf.eu

[20] CORNWELL, T.J., PERLEY, R.A., GOLAP, K. and BHATNAGAR, S. (2004), *RFI Excision in synthesis imaging without a reference signal*, NRAO EVLA Memo, 86. https://library.nrao.edu/public/memos/evla/legacy/evlamemo86.pdf

[20a] DESHPANDE, A. A. *et al*., (2011), *Work on phased array feeds for radio telescopes and their use in RFI mitigation / spatial filtering (nulling)*.

[21] DELLER, A. [2010], *Software correlators as testbeds for RFI algorithms*, PoS (RFI2010) 035.

[22] DONG, W., JEFFS, B.D. and FISHER, J.R. (2005), *Radar interference blanking in radio astronomy using a Kalman tracker*, Radio Sci., Vol. 40, 5, RS5S04.

[23] ELLINGSON, S.W. (2003), *Beamforming and interference cancelling with very large wideband arrays, IEEE Trans. Antennas and Propagation*, Vol. 51, pp. 1338-1346.

[24] ELLINGSON, S.W. (2005), *Introduction to special section on mitigation of radio frequency interference in radio astronomy*. Radio Sci., Vol. 40, 5, RS5S01.

[25] ELLINGSON, S.W., BUNTON, J.D. and BELL, J.F. (2001), *Removal of the GLONASS C/A signal from OH spectral line observations using a parametric modeling technique*. Astrophys. Journ., Supplement 135, 87.

[26] ELLINGSON, S.W. (2002), *Capabilities and limitations of adaptive canceling for microwave radiometry*, Proc. IEEE Geoscience (Remote Sensing Symposium) 3, 1685.

[27] ELLINGSON, S.W. and HAMPSON G.A. (2002), *A subspace-tracking approach to interference nulling for phased array-based radio telescopes*. IEEE Trans. Antenn. and Prop., Vol. 50, 1, pp. 25-30.

[28] ELLINGSON, S.W. and HAMPSON G.A. (2003), *Mitigation of radar interference in L-band radio astronomy*. Astrophysical Journal Supplement, 147, 167.

[29] FELIACHI, R., WEBER, R. and BOONSTRA, A-J. (2009), *Cyclic Spatial Filtering in Radio Astronomy: Application to LOFAR Data*, EUSPICO'09, Glasgow, UK.

[30] FELIACHI, R., WEBER, R. and BOONSTRA, A-J. (2010), *Cyclo-stationarity for phased array radio telescopes*, PoS (RFI2010) 033.

[31] FISHER, J.R., ZHENG, Q., ZHENG, Y., WILSON, S.G. and BRADLEY, R.F. (2005), *Mitigation of pulsed interference to redshifted HI and OH observations between 960 and 1 215 MHz*. AJ 129, 2940.

[32] FRIDMAN, P.A. (1996), *Proc. 8th IEEE Statistical Signal and Array Processing*, p. 264.

[33] FRIDMAN, P.A. (2001), *RFI excision using a higher order statistics analysis of the power spectrum*, Astronomy and Astrophysics, 368, 369.

[34] FRIDMAN, P.A. (2005), *RFI mitigation with phase-only adaptive beamforming*, RadioSci. 40, 2.

[35] FRIDMAN, P.A. (2009), *Robust Correlators*, Astronomy and Astrophysics, 502, 401.

[36] FRIDMAN, P.A. (2010), *Statistically Stable Estimates of Variance in Radio Astronomy Observations as Tools for Radio-Frequency Interference Mitigation*, Astronomical Journal 135, 1810.

[37] FRIDMAN, P.A. and BAAN, W.A. (2001), *RFI mitigation methods in radio astronomy*, Astronomy and Astrophysics, 378, 327.

[38] FLÖER, L., WINKEL, B. and KERP, J. (2010), *RFI Mitigation for the Effelsberg-Bonn HI survey (EBHIS)*, PoS (RFI2010) 042.

[39] GARY, D.E., LIU, Z. and NITA, G.M. (2010), *A Wideband Spectrometer with RFI Detection*, Publications of the Astronomical Society of the Pacific, 122, 560.

[40] HANSEN, C.K., WARNICK, K.F., JEFFS, B.D., FISHER, J.R. and BRADLEY, R. (2005), *Interference mitigation using a focal plane array*, Radio Sci., Vol. 40, 5, RS5S15.

[41] HARP, G.R. (2005), *The ATA digital processing requirements are driven by rfi concerns*, Radio Science, Vol. 40, 5, RS5S18.

[42] HAYKIN, S. (2001), *Adaptive Filter Theory*, 4th Edition, Prentice Hall.

[43] JEFFS, B.D., LI, L. and WARNICK, K.F. (2005), *Auxiliary antenna-assisted interference mitigation for radio astronomy arrays*. IEEE Trans. Signal Proces. Vol. 53, 2, p. 439.

[44] JEFFS, B.D., and WARNICK, K.F. (2008a), *Signal processing for phased array feeds in radio astronomical telescopes*, IEEE Journal of Selected Topics in Signal Processing, Vol. 2, No. 5, pp. 635-646.

[45] JEFFS, B.D., and WARNICK, K.F. (2008b), *Bias corrected PSD estimation for an adaptive array with moving interference*, IEEE Transactions on Signal Processing, Vol. 56, No. 7.

[46] JEFFS, B.D., and WARNICK, K.F. (2009), *Spectral bias in adaptive beamforming with narrowband interference*, IEEE Transactions on Signal Processing, Vol. 57, No. 4, Apr., 2009, pp. 1373-1382.

[47] KALBERLA, P. (2010), *RFI mitigation of the Parkes Galactic All Sky Survey (GASS)*, PoS (RFI2010) 038.

[48] KATZ, C.A. (2003), *A Survey for transient astronomical radio emission at 611 MHz*, Publications of the Astronomical Society of Australia, 115, 675.

[49] KEATING, G., BAROTT, W.C. and WRIGHT, M. (2010), *Automated calibration and imaging with the Allen Telescope Array*, Proc. SPIE 7740, 39.

[50] KESTEVEN, M. (2005), *Adaptive filters revisited: radio frequency interference mitigation in pulsar observations*, Radio Sci., Vol. 40, 5, RS5S06.

[51] KESTEVEN, M. (2010), *Overview of RFI mitigation methods in existing and new systems*, PoS (RFI2010) 07(https://doi.org/10.22323/1.107.0007).

[52] KOCZ, J., BRIGGS, F.H. and REYNOLDS, J. (2010), *Radio frequency interference removal through the application of spatial filtering techniques on the Parkes multibeam receiver*, AJ 140, 2086.

[53] KOGAN, L. & OWEN, F. (2010), *RFI Mitigation in AIPS: The New Task UVRFI*, PoS (RFI2010) 037 (https://doi.org/10.22323/1.107.0037).

[54] LANDON, J., JEFFS, B.D. and WARNICK, K.F. (2011), *Model-Based Subspace Projection Beamforming for Deep Interference Nulling, IEEE Transactions on Signal Processing*, 60 (3) 1215.

[55] LANDON, J., et al. (2010), *Phased Array Feed Calibration, Beamforming, and Imaging*, AJ 139, 1154-1167.

[56] LANE, W.M. *et al*. (2005), *Postcorrelation radio frequency interference excision at low frequencies*, Radio Sci., Vol. 40, 5, RS5S05.

[57] LESHEM, A., and VAN DER VEEN, A.-J. (2000), *Radio-astronomical imaging in the presence of strong radio interference, IEEE Trans. Inf. Theory*. Vol. 46, No. 5, pp. 1 730-1 747.

[58] LESHEM, A., VAN DER VEEN, A.-J. and BOONSTRA, A.-J. (2000), *Multichannel interference mitigation techniques in radio astronomy*, Astrophysic al Journal Supplement, 131, 355.

[59] LIBERTI, J.C. and RAPPAPORT, T.S. (1999), *Smart Antennas for Wireless Communications: IS-95 and Third Generation CDMA Applications*, Prentice-Hall.

[60] MIDDELBERG, E. (2006), *Automated Editing of Radio Interferometer Data with Pieflag*, Australia, 23, 64.

[61] NAGEL, J.R., WARNICK, K.F., JEFFS, B.D., FISHER, J.R., BRADLEY, R. (2007), *Experimental verification of radio frequency interference mitigation with a focal plane array feed*, Radio Science. Vol. 42, No. RS6013.

[62] NIAMSUWAN, N., JOHNSON, J.T. and ELLINGSON, S.W. (2005), *Examination of a simple pulse-blanking technique for radio frequency interference mitigation*, Radio Sci. Vol. 40, 5, RS5S03.

[63] NIGRA, L., LEWIS, B.M., EDGAR, C., *et al*. (2010), *A turn-key concept for active cancellation of the Global Positioning System L3 signal*, PoS (RFI2010) 025 (https://doi.org/10.22323/1.107.0025).

[64] NITA, G.M., GARY, D.E., LIU, Z., HURFORD, G.J. and WHITE, S.M. (2007), *Radio Frequency Interference Excision Using Spectral Domain Statistic*, Publications of the Astronomical Society of the Pacific, 119, 805.

[65] NRQZ (1958), *National Radio Quiet Zone*. https://go.nrao.edu/nrqz

[66] OFFRINGA, A.R., *et al*. (2010), *Post-correlation radio frequency interference classification methods*, Monthly Notices of the Royal Astronomical Society, 405, 155.

[67] OFFRINGA, A.R., DE BRUYN, A.G., and ZAROUBI, S. (2012), *Post-correlation techniques for off-source and RFI removal*, Monthly Notices of the Royal Astronomical Society, 422, 563.

[68] POULSEN, A.J. (2003), *Real-time adaptive cancellation of satellite interference in radio astronomy*. Masters Thesis, Brigham Young University.

[69] PRCZ (1998), *Puerto Rico Coordination Zone*. https://go.nrao.edu/prcz

[70] RAZA, J., BOONSTRA, A.-J., and VAN DER VEEN, A.J. (2002), *Spatial filtering of RF interference in radio astronomy*. IEEE Signal Proc. Lett. Vol. 9, 2, pp. 64-67.

[71] ROGERS, A.E.E., PRATAP, P., CARTER, J.C. and DIAZ, M. (2005), *Radio frequency interference shielding and mitigation techniques for a sensitive search for the 327 MHz line of Deuterium*, Radio Science. Vol. 40, No. 5.

[72] ROSHI, D.A. (2002), *Cancellation of TV interference, NRAO Electronics Division Technical Note* 193. https://library.nrao.edu/public/memos/edtn/EDTN_193.pdf

[73] RFI2004 (2004), *Workshop on Mitigation of Radio Frequency Interference in Radio Astronomy*, July 16-18, 2004, Penticton, BC, Canada (https://doi.org/10.1029/2005RS003268).

[74] SEKHAR, S & ATHREYA, R., *Two Procedures to Flag Radio Frequency Interference in the UV Plan*, Astronomical Journal, 156, Issue 1, article id 9, 8 pp. (2018).

[75] SIROTHIA, S.K. *et al*. (2009a), *Deep low-frequency observations with the Giant Metrewave Radio Telescope: a search for relic radio emission*, Monthly Notices of the Royal Astronomical Society, 392, 1403.

[76] SIROTHIA, S.K. *et al*. (2009b), *325-MHz observations of the ELAIS-N1 field using the Giant Metrewave Radio Telescope*, Monthly Notices of the Royal Astronomical Society, 395, 269.

[77] SMITH, E. T. (2022), *Impact of Radio Frequency Interference and Real-Time Spectral Kurtosis Mitigation. Graduate Theses, Dissertations, and Problem Reports.* 11467. https://researchrepository.wvu.edu/etd/11467

[78] THOMPSON, A.R. (1982), *The response of a radio-astronomy synthesis array to interfering signals*. IEEE Trans. Antenn. and Prop. Vol. 30, 3, pp. 450-456.

[79] TUCCARI, G., CADDEMI, A., NICOTRA, G. and CONSOLI, F. (2004), *Cryogenic Filters for RFI Mitigation in Radioastronomy*, Proc. 7th European VLBI Network Symposium, Toledo, Spain.

[80] VAN ARDENNE, A., SMOLDERS, B., and HAMPSON, G. (2000), *Active adaptive antennas for radio astronomy: results from the R&D program on the Square Kilometer Array*, Proc. SPIE 4015, 420.

[81] VAN DER Tol, S. & VAN DER Veen, A.-J. (2005), *Performance Analysis of Spatial Filtering of RF Interference in Radio Astronomy*, IEEE Signal Proc. 53, 3, 896.

[82] VAN TREES, H. (2002), *Detection, Estimation and Modulation, Part IV: Optimum Array Processing*, John Wiley and Sons.

[83] VAN VEEN, B.D. and BUCKLEY, K.M. (1988), *Beamforming: A versatile approach to spatial filtering, IEEE Acoustic, Speech and Signal Processing*.

[83a] Warnick, K. F.; Maaskant, R.; Ivashina, M. V.; Davidson, D. B. (2009), *High-sensitivity phased array feeds for radio astronomy.*

[84] WEBER, R., CLERC, V., DENIS, L. and ROSOLEN, C. (2002), *Robust Receiver for RFI Mitigation in Radio Astronomy*, Proc. of XXVII GA (URSI Maastricht), 144, 2002. http://scholar.google.com/scholar?cluster=5383997688886129351&hl=en&as_sdt=0,5&sciodt=0,5

[85] WEBER, R., FAYE, C., BIRAUD, F. and DANSOU, J. (1997), *Spectral detector for interference time blanking using a quantized correlator*, Astronomy and Astrophysics Supplement, 126, 161.

[86] WEBER, R., ZARKA, P., RYABOV, V.B, *et al*. (2007), *Data Preprocessing for Decametre Wavelength Exoplanet Detection: an Example of Cyclostationary RFI Detector*, EUSPICO'07, Poznan, Poland.

[87] WIJNHOLDS, S.J., BREGMAN, J.D. and BOONSTRA, A-J. (2004), *Sky noise limited snap shot imaging in the presence of rfi with LOFAR's initial test station*, RFI2004, Penticton, Canada.

[88] ZHENG, Q., ZHENG, Y., WILSON, S.G., FISHER, J.R. and BRADLEY, R.F. (2005), *Excision of distance measuring equipment interference from radio astronomy signals*, Astronomical Journal, 129, 2933.

List of acronyms and abbreviations

ALMA	Atacama large millimetre array
ANC	Adaptive noise cancellation
CSIRO	Commonwealth scientific and industrial research organisation
DME	Distance measurement equipment
FFT	Fast Fourier transform
FPA	Focal plane array

GBT	Green bank telescope
GLONASS	Global navigation satellite system
GMRT	Giant metrewave radio telescope
GPS	Global positioning system
GSO	Geosynchronous orbit
INR	Interference-to-noise ratio
LCMV	Linearly constrained minimum variance
LEO	Low Earth orbit
LOFAR	Low-frequency array
MWRQZ	Mid-west radio quiet zone
NAIC	National Astronomy and Ionosphere Center
NRAO	National Radio Astronomy Observatory
NRQZ	National radio quiet zone
ODS	Operational data sharing
OOBE	Out-of-band emissions
PFD	Power flux-density
PRCZ	Puerto Rico coordination zone
RA	Radio astronomy
RFI	Radio frequency interference
RT	Radio telescope
SKAO	Square kilometre array observatory
SNR	Signal-to-noise ratio
SOI	Signal-of-interest
SpB	Spectral bank
SW	Software
UT	User terminal
VLA	Very large array
VLBA	Very long baseline array
VLBI	Very long baseline interferometry
WIDAR	Wideband interferometric digital architecture
WSRT	Westerbork synthesis radio telescope

Annex 1

First results related to Boresight Avoidance method testing between the NRAO Green Bank Telescope and a non-geostationary orbit (non-GSO) satellite system

The first successful demonstration of the "telescope boresight avoidance" technique was completed in 2024 in the United States of America between the National Radio Astronomy Observatory (NRAO) and a non-GSO system provider.

A1.1 Executive summary

This partnership has been engaged in coordinated testing efforts since Fall 2021, including conducting experiments on different interference avoidance schemes for the Karl G. Jansky Very Large Array (VLA) in New Mexico, and the Green Bank Telescope (GBT) inside the National Radio Quiet Zone in West Virginia and the Very Long Baseline Array (VLBA). The satellite system is capable of avoiding direct illumination of telescope sites with their adaptive tasking to point downlink beams away from RAS station. Nevertheless, even satellites operating in this mode can potentially emit power through their sidelobes into the telescope's receiver system if they pass close to the telescope's main beam at the boresight. For additional protection, the system satellites can either momentarily redirect (outer avoidance) or completely disable their downlink channels while they pass within a defined angular separation threshold from the telescope's boresight (inner avoidance). This method is referred to as "telescope boresight avoidance." In two separate experiments conducted since Fall 2023, an arrangement was made to have the GBT observe a fixed right ascension/declination position in the sky, chosen to have a large number of close-to-boresight satellite passages. Preliminary analysis from these two experiments illustrates the feasibility of these avoidance methods to significantly reduce, the negative impact of close-to-boresight satellite passages. Importantly, these experiments demonstrate the value of continuing cooperative efforts between NRAO and satellite operators, and expanding cooperation between the radio astronomy and satellite communities more generally.

An overview about the various exclusion zone sizes and boresight avoidance parameters if provided in Table A1-1.

TABLE A1-1

Overview on exclusion zone and boresight avoidance parameters in the experiments

Experiment	Tx channels	Exclusion zone size [1] (km)	Inner BSA separation angle [2] (degree)	Outer BSA separation angle [3] (degree)
1	7–8	~15 [4]	Inactive	Inactive
	3–8	~100	Inactive	Inactive
	1–2	180	Inactive	Inactive
2	1–8	~15	0.5	2
Before/after 2	3–8	~15	Inactive	Inactive

[1] Three grid cells centred on the RAS site.

[2] Satellite power switched off.

[3] Satellite beam pointed away from RAS site by more than 180 km.

[4] Only certain mobile user terminals were allowed adjacent to three inner exclusion grid cells.

A1.2 Introduction

In the Ku-band downlink, the satellite operator transmits in eight 250 MHz wide channels. The satellites adjust transmitting power using phased-array beams, accounting for spreading loss and transmitting antenna gain to achieve a target power flux density (PFD) on the ground at each User Terminal (UT) of −146 dBW/m^2/4 kHz.

Since Fall 2021, NRAO has conducted two types of tests with the satellite operator: coordinated and uncoordinated. The former requires formal prearrangement at a given time (typically 48 hours ahead of the scheduled observation) and a pointing direction for the telescopes to intersect with a specific group of satellite passages, as informed by the satellite operator. The latter does not involve input from the satellite operator; NRAO schedules periodic observations on the telescopes at the same pointing position to assess the evolving impact of the satellite's downlink signals during normal operation. The first coordinated experiment took place in Fall 2021 with the testing of a satellite user terminal (UT) at several locations near the VLA in Socorro, NM. This experiment showed clearly that the major RFI issue posed by the UTs was not their uplink signals (14.0-14.5 GHz), but the downlink signals from satellite to ground. In an effort to monitor and evaluate the impact of these space-to-ground transmissions (10.7-12.7 GHz), NRAO worked to install ~60 UTs on the Alamo Navajo Indian Reservation (T'iistsoh) located about 25 miles northeast of the VLA and began monthly uncoordinated tests (still ongoing). Early results of this experiment indicate minor impacts of the Starlink transmissions.

Additionally, the impacts of direct site illumination were conducted through a series of coordinated tests in April and July of 2023. The satellite systems adaptive beam tasking placed their downlink beams to fully illuminate the cells in the U.S. National Radio Quiet Zone (NRQZ). In the April test, the GBT detected a large signal while the telescope was pointed at an elevation of 25 degrees, and pointing to the north. Subsequent analysis of the satellites ephemeris, computed from publicly available two-line elements (TLE), in the vicinity of the GBT's boresight (Fig. A1-1) verified that this large signal was the result of a satellite passing very close to the GBT's boresight at that moment. Since the satellites are at LEO altitudes, the downlink signal only intersects with the GBT's narrow main beam for a short amount of time, on the order of a few tenths of a second.

Recently, NRAO has been developing an autonomous telescope self-reporting system, the Operational Data Sharing (ODS; Nhan et al. 2024) system, to provide near real-time telescope operational information queryable by satellite operators to be incorporated into their satellite tasking algorithms, including some of the telescope avoidance schemes. The ODS data will be frequently updated, ideally refreshed every minute, to allow satellite systems to have awareness of the pointing coordinates and observing frequencies of the VLA and GBT. The boresight avoidance experiments described in this study played a key role in providing preliminary design requirements for the ODS system.

FIGURE A1-1

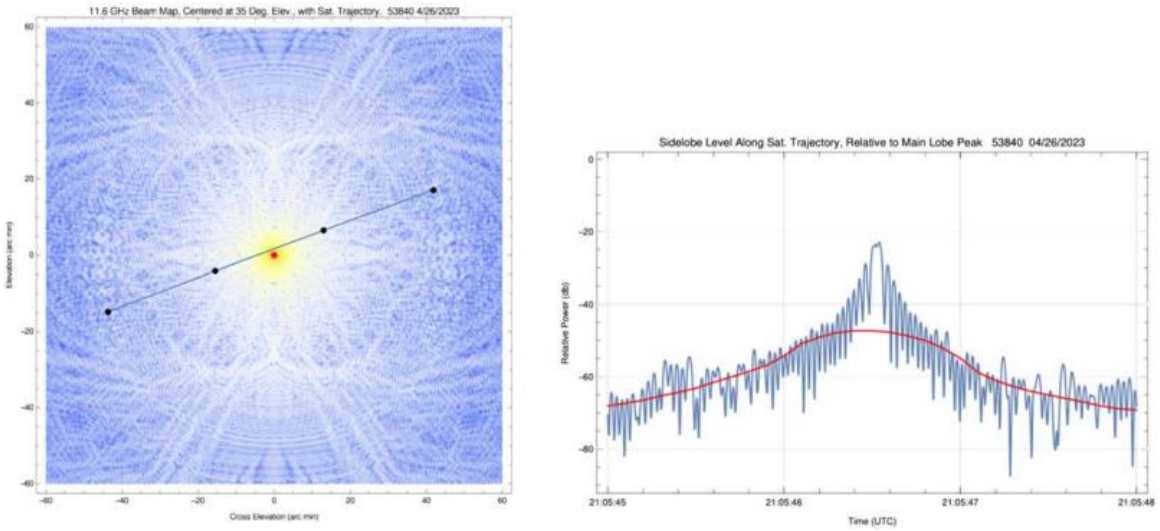

(Left) The simulated GBT beam map at 11.6 GHz, centred at the single dish antenna's elevation (y-axis) and cross-elevation (x-axis) angles, which coincide with the azimuth and altitude angles of the satellite's trajectory, respectively, at the time of observations on April 26, 2023. The black dots indicate the orbital position of a satellite at 1 second intervals, corresponding to the 1 second integration time of the GBT observation, computed from public TLE. Note that this image covers a 2 degrees by 2 degrees square on the sky. (Right) Profile plot of the simulated GBT's bam in relative power in decibels at 11.6 GHz (blue) and its 1 second moving averaged value (red curve).

The coordinated experiments described in this study were carried out on 2023 October 25 (Experiment #1) and 2024 February 19 (Experiment #2). The observational parameters for the two experiments were identical, covering the downlink frequencies in four frequency bands and excluding the uplink bands. For both experiments, the GBT was outfitted with an upgraded X-band receiver (~8-12 GHz; Morgan et al. 2024) to make spectral measurements with the VEGAS6 backend in four overlapping 1.5 GHz wide spectral windows centred at: 9.75, 10.5, 11.25, and 12 GHz, with a resolution bandwidth (RBW) of ~91.6 kHz. These bands are, respectively, denoted as spectral bank (SpB) A, B, C, and D. As part of the coordination, the satellite system's engineering team provided a specified telescope pointing to track in equatorial coordinates (R.A./decl.) over a given UTC time window to schedule an observation of the telescope beforehand. The telescope pointing was chosen to be a position that would result in a large number of close-to-boresight encounters using predicted satellite ephemeris (Fig. A1-2). The satellite operator team also provided a list of satellites with the estimated time when their angular separation from boresight ($\Delta\theta_{bs}$) would be the smallest, based on their ephemeris. Satellite positions provided by the satellite operator were consistent with those independently derived from the public TLE. In each experiment, the telescope observing script was executed manually in real time using the GBT's AstrID7 and CLEO8 user interface software. Each observation consisted of two main steps. This procedure was followed by the main observation sequence with recorded data grouped into multiple scans, each accumulating 10 minutes' worth of 1-second-long integrated spectra, for a total of 600 spectra per scan. Although the VEGAS backend can sample spectra with a much shorter time interval for high time resolution observation, most observations done on the GBT are commonly observed at 1 second integration or longer for better signal-to-noise ratio (SNR). On rare occasions, such as when doing pulsar observation, the observers would store spectra at a sub millisecond scale. Follow-up observations are planned at such a fine timescale to more accurately track the downlink signal from the fast-moving LEO satellites. Additionally, since obtaining the absolute flux calibration was not the priority in these tests, also due to the fast transition of the satellite passages over the telescope, no time was allocated to observe a stronger astronomical flux density calibrator.

FIGURE A1-2

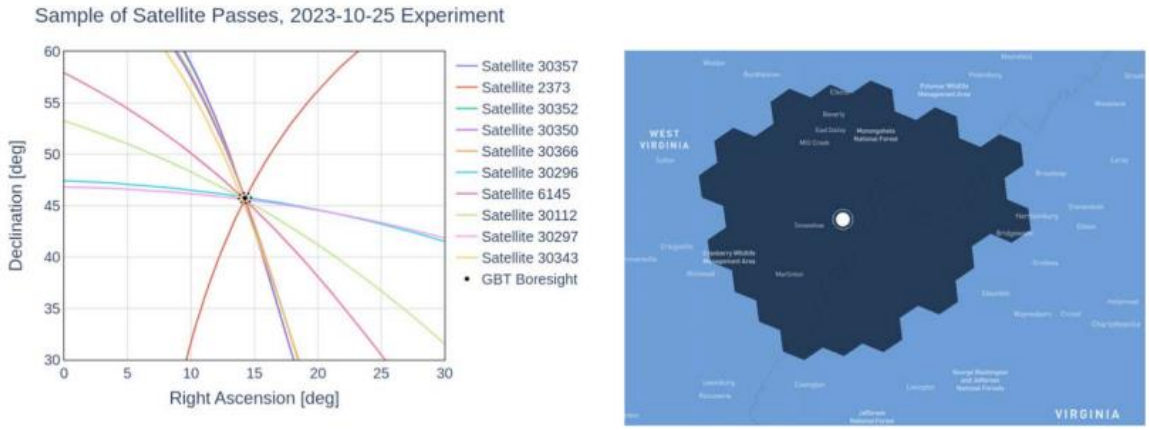

(Left) An example of the experimental setup for the 2023 October test, having the GBT track a fixed pointing at a sky region of (R.A.,decl.) = (14.26 deg, 45.75 deg), where a large number of satellite passages congregate within our observing window. The dashed circle indicates the 0.5 deg. angular distance threshold from the GBT's boresight. (Right) Service cells (dark blue), based on hexagonal hierarchical geospatial indexing system, currently being voluntarily excluded by the satellite system operator for fixed-address UTs within the NRQZ.

Experiment #1 – Boresight avoidance deactivated

This observation started at around 22:09 UTC. The telescope took the first 17 minutes to slew to the prearranged pointing position at (R.A., decl.) = (14.257°, 45.745°) = (00h 57m 1.6s, +45d 44m 43.00s). The auto-peak scan used the calibrator source 1824 + 5651 (1.15 Jy at 9.0 GHz) at 5.3° away from the prearranged pointing to determine the focus correction of −9.59 mm and (azimuth, elevation) offset of (0.1660°, 0.1885°). This telescope pointing was provided by the satellite operator to be a position that would result in 52 close-to-boresight encounters, ranging from 0.06° to 2.96° from the telescope's boresight. The main observation started at 22:25 UTC and concluded at 23:29 UTC.

During this experiment, the satellite system (as it usually does) excluded the three cells located closest to the Green Bank Observatory (GBO), in order to avoid direct illumination of the GBT, but was available to serve mobile units (UTs for RVers and campers) using Channels 7 and 8 only within cells outside the three excluded ones. Also, the satellite system excluded the illumination of any registered UTs in neighbouring cells within the NRQZ listed as "not served" (Fig. A1-2, right panel). A subset of satellites equipped with downlink capability in Channels 1 and 2 are designated with five-digit identification numbers starting with a "3." These satellites were enabled to downlink in all eight Channels during this test, while another subset of satellites were only capable of using Channels 3−8. The only major modification intended for Experiment #1 to normal operations was the use of Channels 1 and 2 to serve locations greater than 180 km from the GBO site (approximately the distance between GBO and Washinton, DC). No boresight-avoidance scheme was implemented in this experiment.

Experiment #2 – Boresight Avoidance Activated

This observation started at around 20:08 UTC. The telescope took the first 17 minutes to slew to the pointing at (R.A., decl.) = (90.1°, 55.4°) = (06h 00m 23.9s, +55d 24m 00.00s). The auto-peak scan used the calibrator source 0541 + 5312 (0.77 Jy at 9.0 GHz) located 3.5° away from the prearranged pointing to determine the focus correction of −3.726 mm and (azimuth, elevation) offsets of (0.2911°, −0.0081°). This sky position was chosen so that during the test, there would be 49 close-to-boresight encounters, ranging from 0.17° to 2.97° from boresight. The main observation started at 20:25 UTC and concluded at 21:59 UTC. Experiment #2 had the same parameters as described for Experiment #1; however, this time the satellite network disabled downlink beams from satellites that were scheduled to pass within 0.5° of the GBT's boresight. This boresight angular separation

threshold is experimental and would be subject to change from satellite operator to operator due to their distinct onboard capabilities and service requirements. Before and after the period of this experiment, the satellite network operated normally without any beam avoidance activated nor downlinking with Channels 1 and 2.

A1.3 Results

Differential spectra

The spectral plots shown below were made by computing the difference between the raw spectra recorded at each 1 second long integration and the median value of all the measured spectra. The raw (uncorrected) antenna temperature, $T_{ant}(t, \nu)$, is first estimated as:

$$T_{ant}(t, \nu) = 0.5 T_{cal} \frac{C_{cal-\mathrm{ON}} + C_{cal-\mathrm{OFF}}}{C_{cal-\mathrm{ON}} - C_{cal-\mathrm{OFF}}} \quad (1)$$

where T_{cal} is the internal calibrator temperature, $C_{cal–\mathrm{ON/OFF}}$ are measured raw counts with internal noise diode calibration signal with a switching cycle of 1 Hz injected into the main radio-frequency signal path. Subsequently, the raw flux density, S(t, ν), in Jansky (Jy) was obtained by:

$$S(t, \nu) = \frac{T_{ant}}{G} \quad (2)$$

where the antenna gain $G = 2.84 \eta ap$ [Kelvin Jy−1] is computed by assuming the GBT's aperture efficiency, ηap = 0.71 across the entire band, and assuming no atmospheric correction is needed for the X-band. Since equation (2) assumes the maximum gain of the GBT, this calculation of $S(t, \nu)$ could have underestimated the exact flux density of the satellite's downlink transmission. To remove any potential offset in individual spectra, it is instead evaluated the differential flux density, which is computed as the difference between all the recorded spectra during the observation and their minimum value of the spectra over the observing time,

$$\Delta S(t, \nu) = S(t, \nu) - \min\left[S(t, \nu)\right] \quad (3)$$

where the minimum value of the spectra was chosen to ensure the least possible RFI is present in the reference spectrum. For illustration purposes, Fig. A1-3 shows a subset of spectra recorded in the SpB-C centred at 11.25 GHz, covering the downlink Channels 1–5 and the protected radio astronomy (RA) band between 10.68 and 10.70 GHz. Examples of the GBT spectra recorded at instances when close-to-boresight satellite passages with $\Delta\theta_{bs} \leq 0.5°$ (left panels) and $\Delta\theta_{bs} > 0.5°$ (right panels) are shown. Each panel shows eight spectra of 1 second integration, centred at the time of the closest encounter in a given passage to show the varying signal strength as a satellite orbiting passes through the GBT's main beam. Note that strong narrowband emissions are present at the transitions between channel pairs (Channels 1–2, 3–4, and 5–6) in some of the passages. The nature and a potential fix for these narrowband emissions are discussed below. In contrast to Fig. A1-3, Fig. A1-4 shows the lack of apparent strong broadband emission in Channels 1–5 for the spectra measured for close-to-boresight satellite passages with $\Delta\theta_{bs} \leq 0.5°$. However, as in Experiment #1, strong narrow-band emissions present at the transitions between downlink channel pairs remain even when the boresight avoidance was activated. These narrowband emissions so far do not seem to pose a problem since no induced intermodulation harmonic components or direct power leakage into the RA band at 10.68-10.70 GHz is observed. As part of the collaborative effort, the satellite operator team identified the source of these emission features and devised a software patch to suppress them, which will be validated with follow-up observations. This example demonstrates the importance of coordination and collaboration between passive and active spectrum users, so both parties can resolve such issues in the early development and deployment phases.

FIGURE A1-3

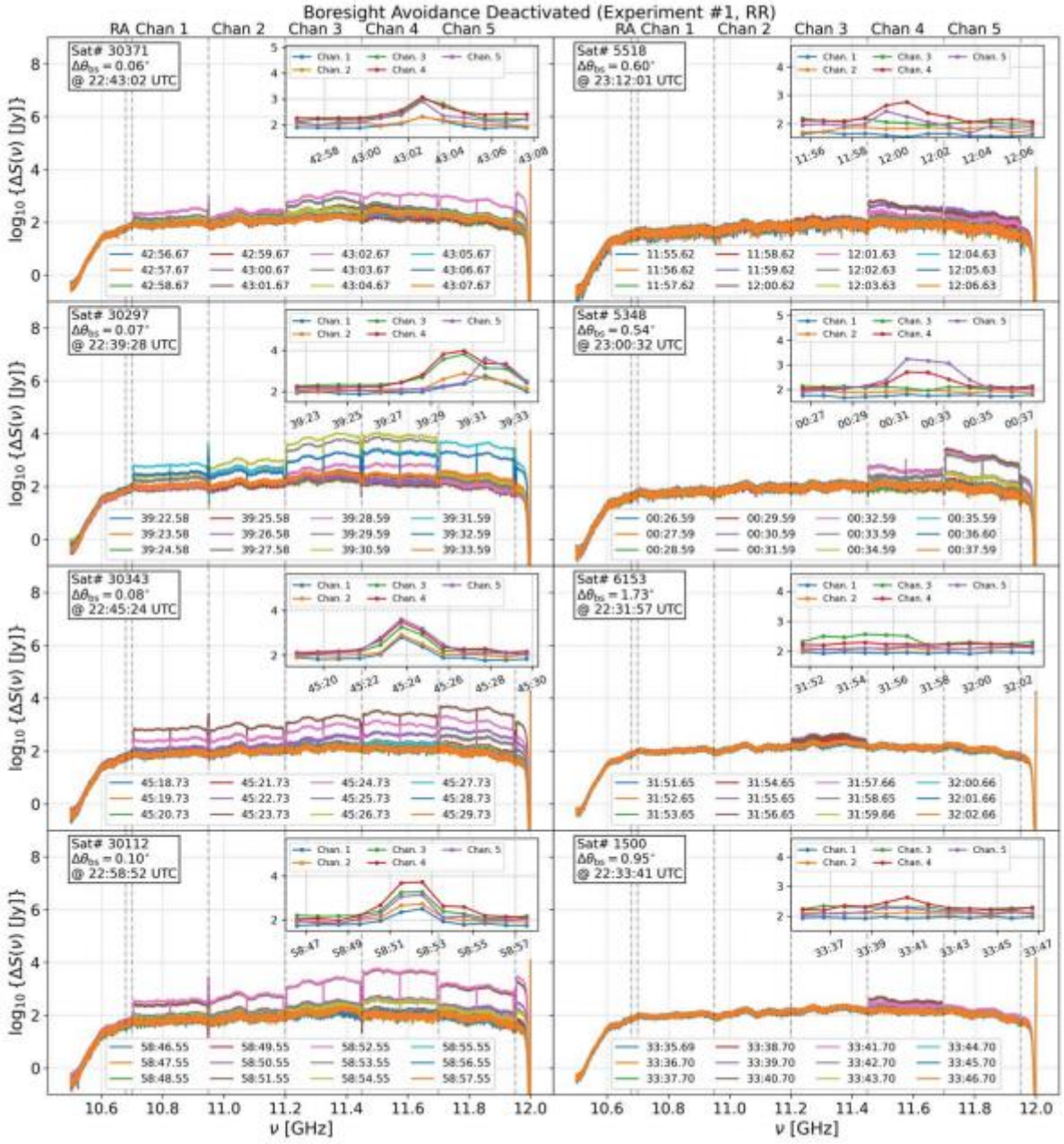

Examples of the spectra from the right-handed circular polarization (RR) recorded in the SpB-C (10.6-12.0 GHz) during Experiment #1, when boresight avoidance was not activated. (Left) Observed spectra recorded with the RA band, downlink Channel 1–5 with satellite passages for $\Delta\theta_{bs} \leq 0.5°$. (Right) Observed spectra recorded in the SpB-C with satellite passages for $\Delta\theta_{bs} > 0.5°$. Satellite passages are shown with the satellite ID and boresight separation in degrees annotated in the legends. Additionally, each panel contains an inset showing the measured power (in logarithmic scale) at one of the passband frequencies within each downlink channel over 12 seconds, centred about the closest passage. In this experiment, the rise and fall of the power correlate with the satellite passages traversing the GBT's main beam, which will be traced out more accurately with higher time resolution in future experiments. Depending on the positioning of the downlink beams relative to the telescope, not all passages peak at the same time as when the satellites are closest to the telescope boresight.

FIGURE A1-4

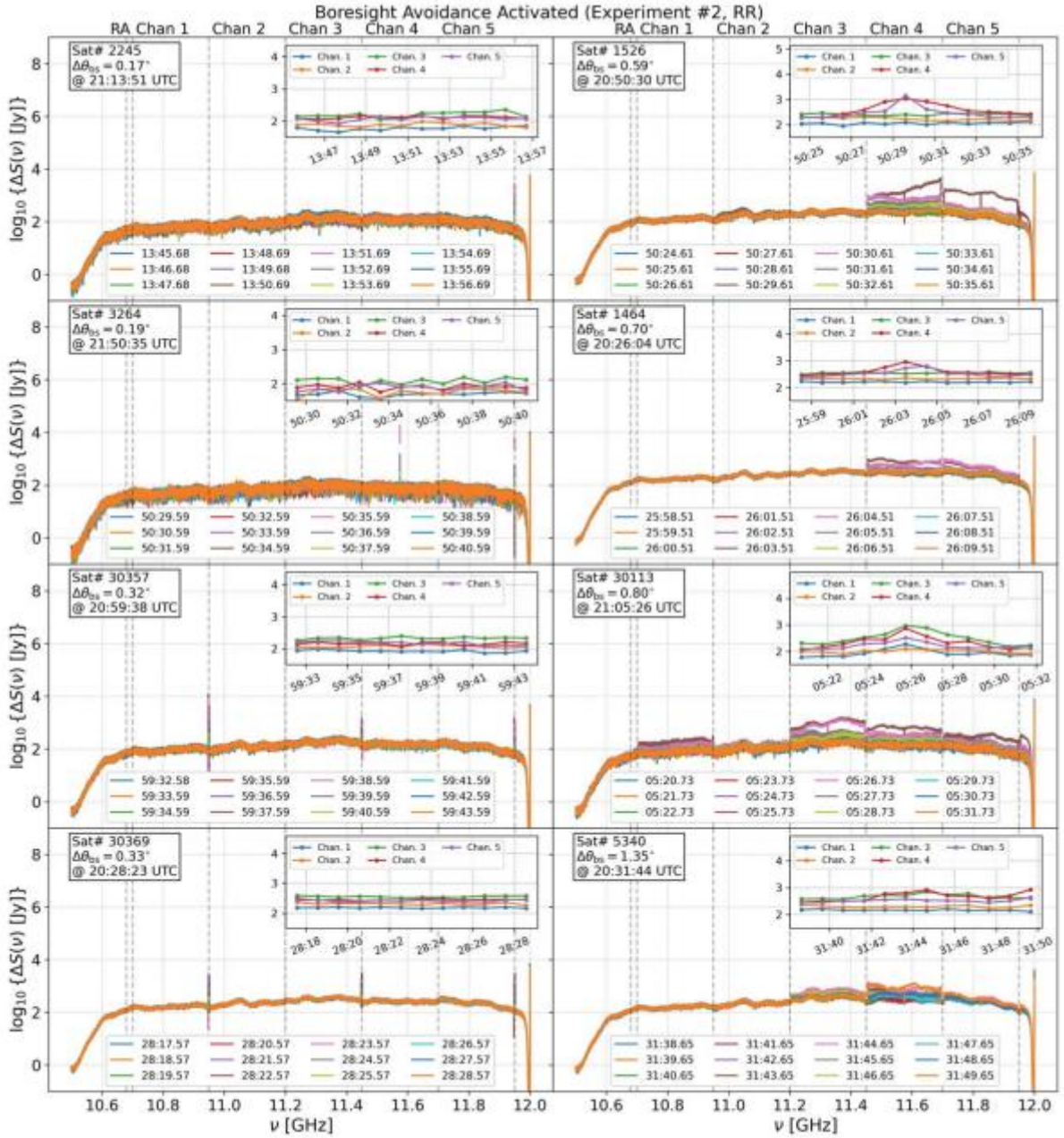

Examples of the spectra from the right-handed circular polarization (RR) recorded in the SpB-C (10.6-12.0 GHz) during Experiment #2, when the boresight avoidance was activated for satellite passages with $\Delta\theta_{bs} \leq 0.5°$. (Left) Observed spectra recorded with the RA band, downlink Channel 1–5 with satellite passages for $\Delta\theta_{bs} \leq 0.5°$. (Right) Observed spectra recorded in SpB-C with satellite passages for $\Delta\theta_{bs} > 0.5°$. Similarly, each panel contains an inset showing the measured power at one of the passband frequencies within each downlink channel over 12 seconds, centred about the closest passage. In this experiment, the rise and fall of the power are only observable for passages with the closest boresight separation outside the 0.5° cutoff.

To quantify the effectiveness of the boresight avoidance, beyond visual inspection of the spectra, two metrics are compared between the two experiments. First, at an expected time for a close satellite passage, the relative SNR between the observed signal level in one of the eight downlink channels and the signal level of a clean channel far from the downlink channels are computed. The clean channel is chosen to be between 9.60 and 9.80 GHz, observed in the SpB-A of the data. This clean channel is denoted as the reference (Ref) signal. Second, the potential spectral leakage from the out-of-band emission (OOBE) into the 10.68-10.70 GHz RA band when there is a nearby satellite downlink in Channels 1–2 (10.70-11.20 GHz) by computing the SNR at the RA band using the same

clean reference signal at 9.6-9.8 GHz is assessed. There are instances that downlink transmission from satellite systems other than the studied satellite operator is present in our data. Hence, only spectra measured at the timestamps when specific satellites were expected to be the closest to the GBT's pointing are considered. Since the downlink channel has a bandwidth of 250 MHz, the median level of the signal across a given downlink channel is used to compute the SNR. Namely, for a given downlink Channel *j*, *SNRj* is defined as:

$$SNR_J = \frac{\text{med}[\Delta S_j(v)]}{\text{med}[\Delta S_{Ref}(v)]} \quad (4)$$

where S_{Ref} is the flux density in the clean reference channels at 9.60-9.80 GHz. The SNR for the RA band is computed in the same manner using the median value of the flux density across the 10.68-10.70 GHz band. If boresight avoidance is activated by the satellite system and working as expected, the observed SNRs in the downlink channels, along with one in the RA band, are close to unity (zero in logarithmic scale) since no transmission is made during the close-to-boresight passages. Our analysis shows that the boresight avoidance is functional and helps to reduce the RFI significantly. In particular, as shown in Fig. A1-5, for passages with $\Delta\theta_{bs} \leq 0.5°$, the SNR for the eight downlink channels in Experiment #1 (left panels) are at least two orders of magnitude higher than the ones in Experiment #2 (right panels) with boresight avoidance activated.

FIGURE A1-5

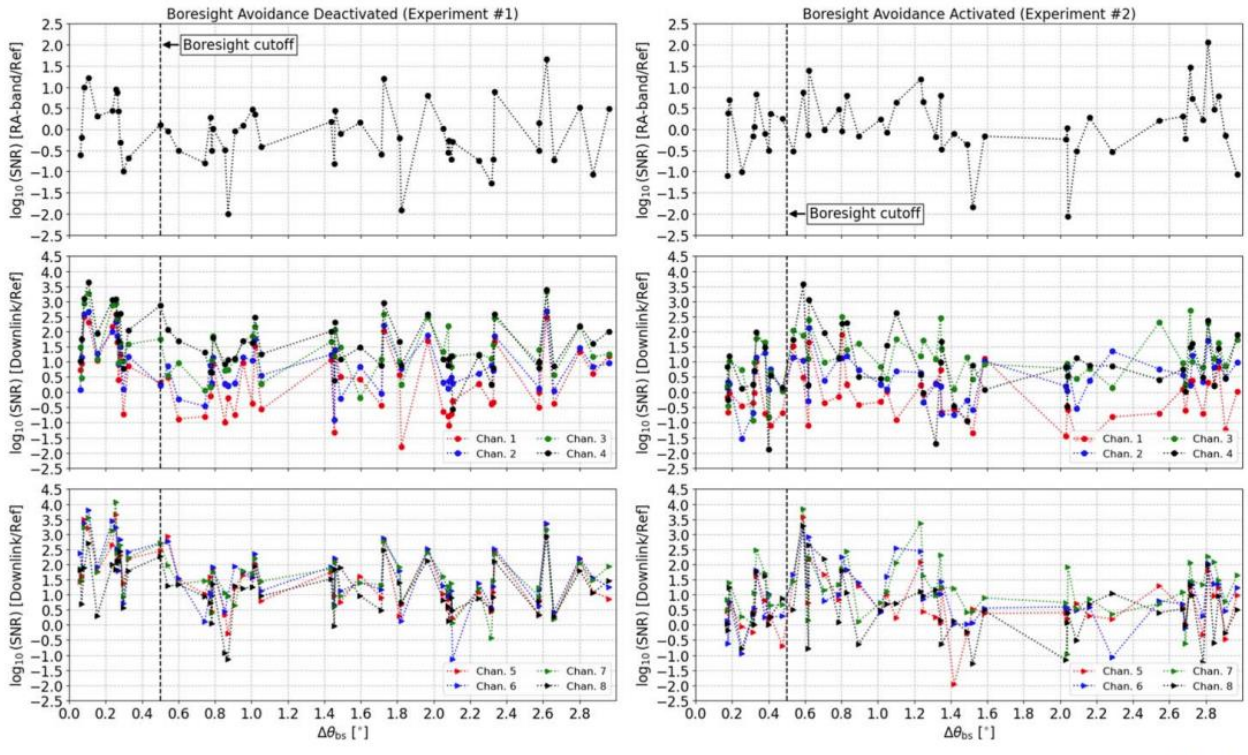

Comparison of SNR (in logarithmic scale) between Experiment #1 (left) and #2 (right). SNR within the boresight separation threshold, $\Delta\theta_{bs} = 0.5°$ (dashed line), is distinctly lower in Experiment #2 when the boresight-avoidance tasking is activated by the satellite system. Each data point represents a unique satellite passage observed during the experiments, with a total of 52 (49) passages observed in Experiment #1 (#2). Note that the SNR for Experiment #2 appears to be higher than the nominal SNR at $\Delta\theta_{bs} = 0.59°$ because a particular satellite passage (Sat #1526 at 20:50:30 UTC, upper right panel of Fig. A1-4) was downlinking in Channel 4, 5, 6, 7 and 8.

A1.4 Discussion and summary

Besides avoiding direct site illumination, one method to protect a telescope from non-GSO satellite transmissions is through adaptive beam tasking that places a satellite's downlink beams far away

from the telescope site when the satellite is within a certain angular separation from the telescope's boresight during observation. For example, a satellite that passes within 2 degrees of boresight could be directed to steer its beams no closer than 180 km from a radio telescope. An additional protection level can be achieved by completely disabling downlink beams from satellites that pass within an even tighter cone of a telescope's boresight during observation. This operational mode would further reduce the chance of a telescope's main beam being illuminated by any satellite's downlink beam, including its inner sidelobes. At the moment, these two mitigation methods are referred to, both separately and collectively, as the "telescope boresight-avoidance" method. This study has, for the first time, demonstrated the feasibility of implementing the telescope boresight-avoidance method between a radio astronomy telescope and a LEO satellite operator through collaborative experiments between NRAO's Green Bank Telescope and the satellite operator. This experiment was made possible by sharing the radio telescope's pointing position and frequency of observation with the LEO satellite operator, who was then able to use this data to mitigate interference in the telescope. The two experiments conducted at the GBT in 2023 October and 2024 February demonstrated:

1 When informed about a telescope's pointing direction and the frequency band being observed, the satellite system is capable of disabling downlink beams for satellite passages close to telescope boresight. While this action is planned for the closest of boresight passages, it is expected that refraining from placing beams near the radio telescope will suffice for most near-boresight passages of consequence.

2 Briefly disabling satellite downlinks as a satellite passes close to boresight can significantly reduce the observed satellite emission in the radio astronomy data, indicated by statistically significant reductions in SNR by two orders of magnitude inside the 0.5° radius.

3 For satellite passages using Channels 1 and 2, although the SNR levels of the RA band between 10.68 and 10.7 GHz in both experiments are approximately unity, a closer inspection suggests a slight increase (about a factor of 3) in signal level in Experiment #1 for passages with $\Delta\theta_{bs} \leq 0.5°$ (Fig. A1-5, top left panel). This potential leakage is no longer an issue when boresight avoidance is in use for close passages (Fig. A1-5, top right panel).

This work has provided critical data for both the NRAO and the satellite operator teams to refine the design parameters of the telescope boresight-avoidance method, such as a boresight degree separation threshold and a satellite's downlink disabling timescale. In particular, feedback for NRAO's development of the autonomous self-reporting ODS system, which will provide near real-time telescope operational data (e.g. pointing coordinate, observing band, observation mode, and duration) to satellite operators to implement similar telescope avoidance schemes in their network algorithms.

While the experimental demonstration of boresight-avoidance methods between the GBT and a LEO operator provides a potentially useful voluntary coordination practice, this does not imply that such techniques are universally applicable, scalable, or operationally sustainable across global satellite constellations. As a technical matter, adaptive beam-steering and boresight avoidance depend on close to real-time exchange of telescope ephemerides, band use, and observation parameters, which may not always be feasible given the dynamic and proprietary nature of both RAS and satellite operations. Furthermore, these methods are not yet proven effective in all interference scenarios (e.g. aggregate sidelobe interference, dynamic scheduling, intermodulation) and is likely to put burden on radio telescope operators in managing a real time radio telescope antenna pointing direction database that is not always feasible (e.g. target-of-opportunity observations). If considered, this technique should be considered supplementary and not used to comply with the single-entry 2% criteria of the Radio Astronomy Service (Recommendation ITU-R RA.1513).

Annex 2

Example of operational data sharing record

In Table A2-1 an example data format is shown for data sharing of telescope operational parameters that includes telescope location, pointing direction, and observing frequency range.

TABLE A2-1

Example data format of an ODS record. For more information, please refer to: *https://obs.vla.nrao.edu/ods/*

Attribute	Type	Format	Example	Description
site_id	String		vla_D	Identifier of the observatory/instrument. In the example '_D' indicates VLA 'D' configuration. The possible 'site_id's for the VLA are: vla_A, vla_A-to-D, vla_D, vla_D-to-C, vla_C, vla_C-to-B, vla_B, vla_B-to-BnA, vla_BnA, vla_BnA-to-A.
site_lat_deg	number	decimal-degrees +/− DD.D	34.07874917	the latitude of the observatory/instrument
site_lon_deg	number	decimal-degrees +/− DDD.D	−107.6177275	the longitude of the observatory/instrument
site_el_m	number	decimal-meters	2124	the elevation of the observatory/instrument
src_id	string		J1056 + 7011	identifier of source/target observed during time interval
src_is_pulsar_bool	boolean		false	true = src is a pulsar, false = src is not a pulsar
corr_integ_time_sec	number		3	correlator integration time in seconds (if 'src_is_pulsar_bool' = false)
src_ra_j2000_deg	number	decimal-degrees	70.88181332916666	right ascension of the source/target
src_dec_j2000_deg	number	decimal-degrees	34.685184469444444	declination of the source/target
src_radius	number	decimal-degrees	0.0034	radius of beam around the source/target
src_start_utc	string	date-time	2023-08-16T15:23:47.000541	start time of this observing interval
src_end_utc	string	date-time	2023-08-16T15:26:16.000723	end time of this observing interval
slew_sec	number		130.8	the time taken for the array to reach the source (counted from 'src_start_utc')
trk_rate_dec_deg_per_sec	number	decimal-degrees per second	0	declination tracking rate of src (if not sideral)
trk_rate_ra_deg_per_sec	number	decimal-degrees per second	0	right ascension tracking rate of src (if not sideral)
freq_lower_hz	number	decimal-Hz	26000000000	lower limit frequency used during this interval
freq_upper_hz	number	decimal-Hz	40000000000	upper limit frequency used during this interval
notes	string		inAdv:True	notes that add context to the data